University of Crete

Department of Biology

MSc Program: Plant Molecular and Applied Biology - Green Biotechnology

"The role of *Arabidopsis thaliana* Kin7/Separase complex (KISC) in light signaling pathways"

A thesis submitted for the degree of Master of Science

by

Anastasia Fragkiadaki

Thesis Committee

Thesis Supervisor: Associate Professor Panagiotis Moschou

Committee Member: Professor Kriton Kalantidis

Committee Member: Professor Kiriakos Kotzabasis

November 2020

Ευχαριστίες

Η παρούσα διπλωματική εργασία δεν θα μπορούσε να ολοκληρωθεί χωρίς τη συμβολή ανθρώπων, οι οποίοι είτε με τις πράξεις τους, είτε απλά με την παρουσία τους, βρέθηκαν δίπλα μου. Με εμπιστεύτηκαν, με συμβούλεψαν, με σήκωσαν τις στιγμές που απογοητεύτηκα – συμβαίνει σε όλους, μου είπαν, εδώ είμαστε-, με ενθάρρυναν (είτε από μακριά είτε από απόσταση μηδενική).

Θα ήθελα πρώτα από όλους, να ευχαριστήσω τον υπεύθυνο καθηγητή της διπλωματικής μου εργασίας, κ. Παναγιώτη Μόσχου, ο οποίος πρωτίστως με εμπιστεύτηκε. Χωρίς να έχω πείρα και φιλόδοξα σχέδια για το μέλλον. Έπειτα, ήταν εκεί για να παρακολουθήσει από την αρχή ως το τέλος την πορεία μου και να με συμβουλέψει -έμαθα μετέπειτα ότι κάτι τέτοιο δεν είναι αυτονόητο-.

Θα ήθελα ακόμη να ευχαριστήσω και όλα τα υπόλοιπα μέλη της τριμελούς μου επιτροπής, τον κ. Κυριάκο Κοτζαμπάση και τον κ. Κρίτωνα Καλαντίδη, που δέχτηκαν να συνεπιβλέψουν την εργασία αυτή, παρά το μεγάλο φόρτο εργασίας που χαρακτηρίζει τη θέση τους. Τους ευχαριστώ και γιατί γνωρίζω ότι όποτε και αν χρειαζόμουν τη βοήθεια τους, θα ήταν εκεί.

Ακόμη, ένα μεγάλο ευχαριστώ από καρδιάς, σε όλα τα μέλη του εργαστηρίου. Ιδιαίτερα στην Άντρια, που επέβλεψε την δουλειά που αποτυπώνεται σε αυτές τις σελίδες και είχε την υπομονή να με εκπαιδεύσει στον «πάγκο», σε χρόνο περιορισμένο, και γνωρίζοντας ότι αρχίζω «από το μηδέν». Ακόμη, ευχαριστώ τον Γιάννη, που μου έμαθε λέξεις-κλειδιά για να περνάμε καλά και ήτανε πάντα γενναιόδωρος με τη λαβίδα του, την Άλεξ, για τις συμβουλές της και την παρέα της στο «μπεντένι δεξιά», την Ειρήνη, που πάντα με ρωτούσε αν χρειάζομαι κάτι, και την Άρτεμις, που στον ελάχιστο χρόνο που συνυπήρξαμε με συμβούλεψε καταλυτικά. Ιδιαίτερα, θα ήθελα να ευχαριστήσω και τη μαμά-Σπυριδούλα (ας μου συγχωρέσει το χαρακτηρισμό, νομίζω είναι εμφανής η χιουμοριστική του διάθεση), όχι μόνο για τη βοήθειά της σε επίπεδο εργαστηρίου, αλλά και γιατί ήταν πάντα εκεί, για όλα εκεί.

Τέλος, θα ήθελα να ευχαριστήσω την οικογένειά μου, η οποία στάθηκε για άλλη μια φορά «βράχος» στα βήματά και στις επιλογές μου. Ακόμη και αν δεν το εκφράζω δυνατά κάποιες φορές, κρατάω πάντα φυλαχτό, την αγάπη και τη στήριξή τους. Αλλά ευχαριστώ και τις φίλες και τους φίλους. Αυτές και αυτούς που τους «εγκατέλειψα» το χρόνο αυτό, αλλά ποτέ δεν ξέχασα την «υπόσχεση» τις κοινής ζωής, και αυτές που βρέθηκαν εδώ μαζί μου, χτίσαμε σχέσεις ουσιαστικές, αλληλοβοηθηθήκαμε και μοιραστήκαμε το ταξίδι (ας με συγχωρήσουν και αυτές για την «αντιαισθητική» γραφικότητα, αλλά τίποτα δεν ήταν πιο σημαντικό από την πολυσήμαντη παρουσία τους).

Abstract

As sessile organisms, plants have developed numerous physiological adaptations, such as light capture optimization. Fluctuations in spectral composition and intensity of incoming sunlight are perceived by a plethora of photoreceptors, responsible for the initiation of a signal cascade, known as light signaling. The evident complexity of the signal network underlines the long evolutionary time plants have gone through, while at the same time, it implies that, despite our growing understanding towards this network, our current knowledge remains incomplete. This study aims to contribute to the better understanding of the light signaling events, through investigating the involvement of a novel complex in light signaling cascade. Specifically, this thesis examined the biological function of Kin7/Separase complex (KISC) under the scope of photobiology, by pursuing two different, yet converging approaches. On the one hand, it included validation of some of the potential protein-protein interactions (PPIs) between KISC and light signaling components. On the other hand, physiological experiments were conducted, using different loss-of-function mutant lines related to KISC, which were phenotypically characterized in response to different light qualities. It was shown that Kinesin7.3 (Kin7.3), a core component of KISC, interacts through its tail domain with one of the major blue-light and UV-A photoreceptors, known as Phototropin1 (PHOT1). Furthermore, KISC was shown to be involved in hypocotyl growth inhibition upon blue light exposure, as well as in phototropism, leaf flattening, and leaf positioning responses. Taken together, the resulting preliminary data suggest that KISC acts in the crossroads of phototropin- and phytochrome-mediated signal transduction. Additionally, my data suggest that KISC constitutes a necessary complex for the autotropism response.

Περίληψη

Τα φυτά, ως ακίνητοι οργανισμοί, έχουν αναπτύξει πολυάριθμες φυσιολογικές προσαρμογές, όπως την βελτιστοποίηση της συλλογής του φωτός. Οι διακυμάνσεις στη φασματική σύνθεση και στην ένταση του εισερχόμενου φωτός, γίνονται αντιληπτές από μία πληθώρα φωτοϋποδοχέων, οι οποίοι είναι υπεύθυνοι για την έναρξη ενός καταρράκτη μετάδοσης σήματος. Η εμφανής πολυπλοκότητα του δικτύου σηματοδότησης, υπογραμμίζει το μακρύ εξελικτικό χρόνο, τον οποίο έχουν διανύσει τα φυτά, ενώ ταυτόχρονα υποδηλώνει ότι, παρά την αυξανόμενη κατανόησή μας πάνω στο δίκτυο αυτό, η επί του παρόντος γνώση παραμένει ελλιπής. Η παρούσα μελέτη είχε ως στόχο να συμβάλλει στην περεταίρω κατανόηση των συμβάντων που εμπλέκονται στα μονοπάτια φωτεινής σηματοδότησης, μέσω της διερεύνησης της συμμετοχής ενός προσφάτως χαρακτηρισμένου συμπλόκου στον προαναφερθέντα καταρράκτη μετάδοσης σήματος. Ειδικότερα, η εργασία εξετάζει τη βιολογική λειτουργία του συμπλόκου Kin7/Separase (KISC) υπό το πρίσμα της φωτοβιολογίας, ακολουθώντας δύο διαφορετικές, ωστόσο συγκλίνουσες, προσεγγίσεις. Από τη μία, περιλαμβάνει την εξακρίβωση ορισμένων από τις πιθανές πρωτεϊνικές αλληλεπιδράσεις μεταξύ του συμπλόκου KISC και συγκεκριμένων συστατικών που εμπλέκονται στο μονοπάτι σηματοδότησης του φωτός. Από την άλλη, διενεργήθηκαν παράλληλα πειράματα φυσιολογίας, στο πλαίσιο των οποίων διαφορετικά μεταλλάγματα απώλειας λειτουργίας, όλα σχετιζόμενα με το σύμπλοκο KISC, χαρακτηρίστηκαν φαινοτυπικά έπειτα από έκθεση σε διάφορες ποιότητες φωτός. Δείχθηκε ότι η πρωτεΐνη Kinesin7.3 (Kin7.3), ένα βασικό συστατικό του συμπλόκου KISC, αλληλεπιδρά μέσω της καρβοξυτελικής της επικράτειας με έναν από τους κύριους φωτοϋποδοχείς για το μπλε φως και την UV-A ακτινοβολία, γνωστού ως Φωτοτροπίνη1 (PHOT1). Επιπλέον, τα στοιχεία που προέκυψαν, υποδεικνύουν την εμπλοκή του KISC στην αναστολή της αύξησης του υποκοτυλίου έπειτα από έκθεση σε μπλε φωτισμό, καθώς και την εμπλοκή του στο φωτοτροπισμό, στην επιπέδωση της φυλλικής επιφάνειας και την υποναστίας. Στο σύνολό τους, τα προκαταρκτικά δεδομένα που προέκυψαν θα μπορούσαν να υποδηλώνουν ότι το σύμπλοκο KISC δρα στη διασταύρωση των δύο μονοπατιών μεταγωγής σήματος: αυτού της φωτοτροπίνης και αυτού του φυτοχρώματος. Επιπλέον, τα δεδομένα μου δείχνουν ότι το KISC αποτελεί ένα απαραίτητο σύμπλοκο για την απόκριση του αυτοτροπισμού.

Περιεχόμενα

Introduction

1.1 KISC complex: regulating microtubule dynamics and cell polarity

Separase (EXTRA SPINDLE POLES, ESP) has an evolutionary conserved role in daughter chromatid separation, based on its function to cleave a subunit of the protein complex cohesin, which is responsible for joining sister chromatids together (Liu & Makaroff, 2006; Yang et al., 2009; Moschou & Bozhkov, 2012). However, separase has been suggested to exhibit additional functions in many systems including plants. In fission yeast, separase mediates DNA repair during interphase (Nagao et al., 2004), while in budding yeast regulates mitotic exit, by indirectly promoting microtubule stability (Queralt et al., 2006). Apart from its mitotic function, Moschou et al. (2013) showed the important role of separase in linking membrane protein trafficking with the cytoskeleton and the polar targeting of the auxin efflux carrier PIN-FORMED2 (PIN2) to the rootward side of the root cortex cells. Specifically, in *rsw4* mutants (*radially swollen 4*, a temperature-sensitive point mutation of the *Arabidopsis thaliana* (At) *At*ESP gene), defects in anisotropic cell expansion were observed, implicating the role of *At*ESP in cell polarity (Figure 1).

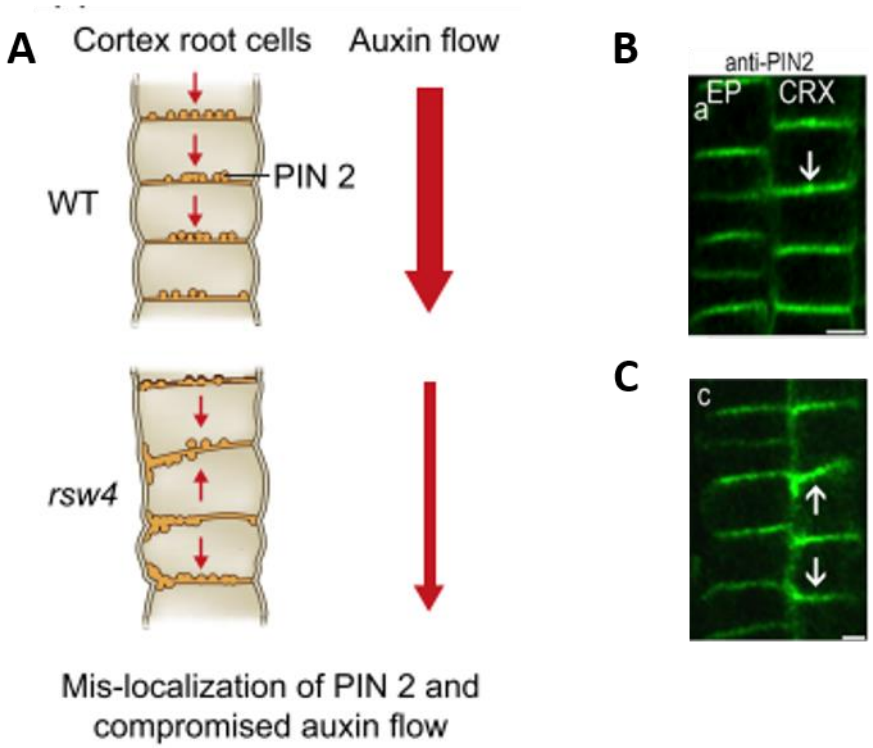

Figure 1. AtESP regulates polar targeting of PINs. (A) ESP loss-of-function in the conditional mutant *rsw4* leads to auxin efflux carrier PIN2 secretion and localization defects, compromising auxin gradient in root cells. WT, wild-type (Liu & Moschou, 2017). (B, C). Immunostaining of PIN2 (green online) in the root tips of wild-type (B) and *rsw4* plants grown at the restrictive temperature. EP, epidermis; CRX, cortex (Moschou et al., 2013)

The N-terminal region of *At*ESP interacts with the C-terminal region of a putative microtubule-based motor (AT3G12020), which belongs to the group 7 (Kin7) of the kinesin superfamily, thus designated as Kinesin 7.3 (Kin7.3). Additionally, it was shown that, in the absence of *At*ESP, Kin7.3-tail domain (Figure 3C) folds over and blocks the motor domain. This effect is inhibited by conformational changes induced by the interaction of AtESP with the tail domain

of Kin7.3 (Moschou et al., 2016). AtESP-Kin7.3 complex, abbreviated as KISC, revealed the mechanism, under which separase associates with microtubules and membrane protein trafficking (Figure 2).

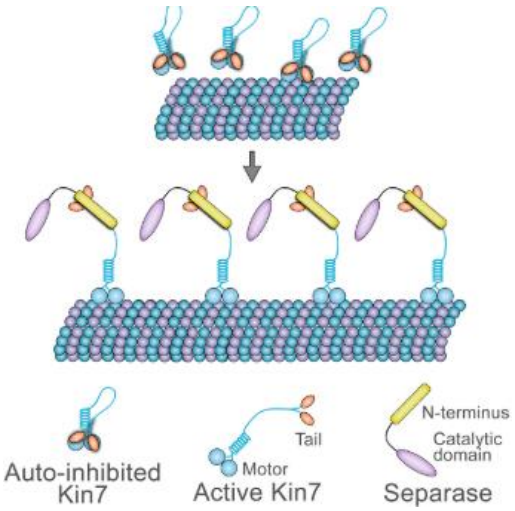

Figure 2. Schematic representation of KISC binding onto microtubules (Moschou et al., 2016)

Kin7.3 belongs to a clade of five *Arabidopsis* proteins together with Kin7.1 (AT1G21730), Kin7.2 (AT2G21380), Kin7.4 (AT4G39050), and Kin7.5 (AT5G06670) (Figure 3A). Furthermore, all members of the Kin7.3 clade show similar domain organization except for Kin7.2 and Kin7.4, which contain a C-terminal RING domain (Figure 3B). Moreover, it was shown that AtESP not only interacts with Kin7.3, but also with Kin7.1 and Kin7.5. Thus, Kin7.1, Kin7.5, and Kin7.3 are likely to be functionally redundant in KISC functions. This hypothesis, was further confirmed: Following the isolation of triple-transfer DNA (T-DNA) insertion mutant *kin7.1kin7.3kin7.5* (abbreviated as *k135*), treatment with the microtubule-depolymerizing drug amiprophos-methyl (APM) revealed an additive effect of individual mutations on the APM-induced inhibition of root growth (Moschou et al., 2016). These data demonstrate the redundant role of Kin7.1, Kin7.3, Kin7.5 in maintaining microtubule stability.

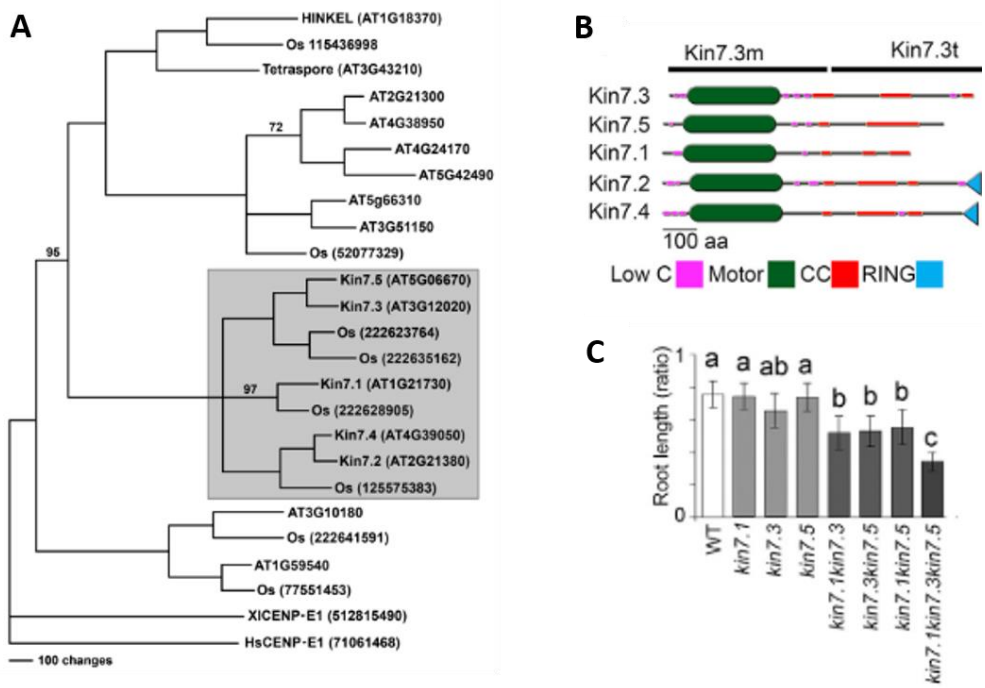

Figure 3. The redundant role of Kin7.3-clade in the maintenance of microtubule stability. (A) *Arabidopsis* Kin7.1, Kin7.2, Kin7.3, Kin7.4 and Kin7.5 form a separate clade within the Kin7 subfamily of kinesins. (B) Domain architecture of Kin7.3 homologs. Low C, low complexity; CC, coiled coil. (C) Effect of microtubule-destabilizing drug APM (10 nM; 6 days) on the root length of WT and mutant seedlings (ratio of values of treated to untreated samples). All figures and description credits: Moschou et al., 2016.

1.2 Linking Kin7.3 to light signaling

Previous published data have revealed that genetic interference with KISC components results in similar phenotypic defects, including disrupted cell division, inhibition of root growth and delayed gravitropic response, caused by mis-localization of the cell polarity marker and efflux carrier of the growth hormone auxin, PIN2 (Moschou et al., 2013; Moschou et al., 2016). Moreover, it is known that knockout mutants of separase *At*ESP are embryonic lethal due to chromosome segregation defects (Z. Liu & Makaroff, 2006). However, all the above-mentioned disrupted cell patterns have been observed in the root system. Yet, little is known about the phenotype characterizing the shoot system of mutant alleles implicated in KISC.

Although the expression pattern of Kin7.3 has been mainly investigated in root tip epidermis and cortical cells, *in silico* data (http://bar.utoronto.ca/*eplan*) indicate that Kin7.3 is also highly expressed in above-ground organs, including cotyledons and rosette leaves of *A. thaliana*. Thus, it is likely that KISC and especially Kin7.3 is also involved in the development of the shoot system during both heterotrophic and autotrophic stage. Moreover, additional unpublished data from Moschou lab, indicate that both *k135* and the single *k7.3* mutant lines display phenotypes in aerial organs. As shown in Figure 4, the aforementioned lines exhibit increased upward leaf movement (hyponasty) compared with the wild type. Indeed, stable transformation in *Arabidopsis* with proKin7.3:GFP- Kin7.3 complements, at least partially, the *k135* phenotype.

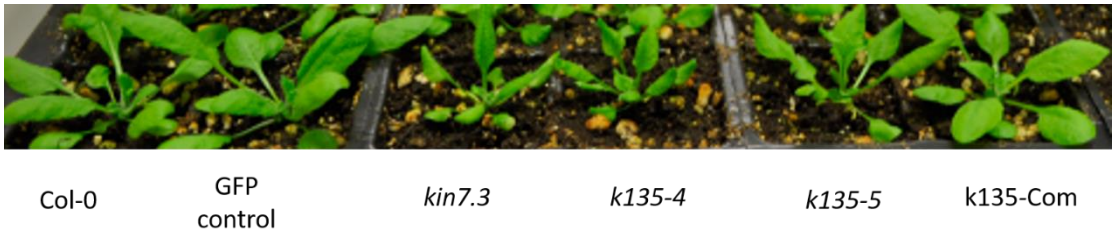

Figure 4. *k7.3* and *k135* mutant lines show upward leaf bending. k135-com: transformed *k135* line with proKin7.3:GFP- Kin7.3 construct; GFP control: transformed Col-0 line with eGFP construct (p7FWGF2). The photo was taken after the end of the photoperiod (end-of-day). Photo and data credits: Panagiotis Moschou and Chen Liu, unpublished.

Hyponasty is one of the numerous developmental adaptations that observed in plants when exposed to shady environments, such as under direct plant canopy shade or along dense vegetation. Such environments are characterized by a reduced Red:Far-Red ratio (R:FR), while the sum of the adaptations triggered are known as Shade Avoidance Syndrome (SAR) (discussed in more detail in section 1.3). Therefore, the question that reasonably arises, is whether KISC acts downstream of R/FR signal perception which mainly initiates from photoreceptors.

Consistently, transcriptome sequencing analysis (RNAseq) highlighted many differentially expressed genes (DEGs) between Col-0 and *k135*. Indeed, around 30 significant Gene Ontology terms (GO terms; FDR<0,05) revealed within biological process, "response to light stimulus" (GO.0009416; FDR = 0.0000121) and "red or far-red light signaling pathway" (GO.0010017; FDR = 0.0307) (Unpublished data). The aforementioned categories were all related to downregulated genes in *k135* mutants, and constitute an additional indication that KISC components are involved in light signaling.

The last evidence supporting the involvement of KISC in light signaling is deduced from the interactome of Kin7.3. Specifically, two proteins that are strongly correlated with the light signaling, emerged as possible interactors of Kin7.3: Phototropin1 (PHOT1) and FAR-RED ELONGATED HYPOCOTYL3 (FHY3) (Moschou lab, unpublished data). PHOT1, is a blue-light receptor evolutionary conserved among photosynthetic algae and flowering plants (Li et al., 2015), discussed in more detail in section 1.4, while FHY3 is a transcription factor essential for phytochrome signaling (Siddiqui et al., 2016; Y. Liu et al., 2019).

Together, all the above-mentioned evidence, formulate the hypothesis that mainly Kin7.3, but also Kin7.1 and Kin7.5 are involved in light signaling. Furthermore, considering the major role of *At*ESP in promoting the biological function of Kin7.3, it would be reasonable to assume the correlation of KISC with the light signaling pathway.

1.3 Shade avoidance response

1.3.1 Morphological and physiological alterations in response to shade

In most ecosystems, plants grow at high densities, which results in shading. The evidently detrimental consequences of the reduction of photosynthetically-active radiation (PAR, 400-700nm), have provided plants with the evolutionary force either to be tolerant to low light

intensities (tolerance strategy), or to generate shade-avoidance responses (escape strategy, e.g. *A. thaliana*) (Casal, 2012; Pierik & De Wit, 2014; Fraser et al., 2016;).

Specifically, plants absorb blue (400–500 nm) and red (635–700 nm) wavelengths through chlorophyll to fuel photosynthesis while reflecting FR wavelengths (700–780 nm) (Figure 5B). Sunlight has an R: FR of approximately 1.2, but neighboring plants can reduce this ratio to as low as 0.1 in deep canopy shade (i.e., canopy closure) (Figure 5A) (Huber et al., 2020). As a result of changed light quality and quantity, either in vertical or horizontal irradiation, shade avoidance syndrome (SAS) is triggered. Generally, shade avoidance responses (SAR) consist of a suite of developmental changes, mainly involving accelerated hypocotyl, petiole and internode elongation, directional growth towards illumination (phototropism), upward movement of leaf or petiole (hyponasty), increased apical dominance (reduced branching), accelerated flowering and in some cases reduced leaf lamina expansion (Figure 5C) (Smith & Whitelam, 1997; Casal, 2012; Roig-Villanova & Martínez-García, 2016; Ballaré & Pierik, 2017; Huber et al., 2020).

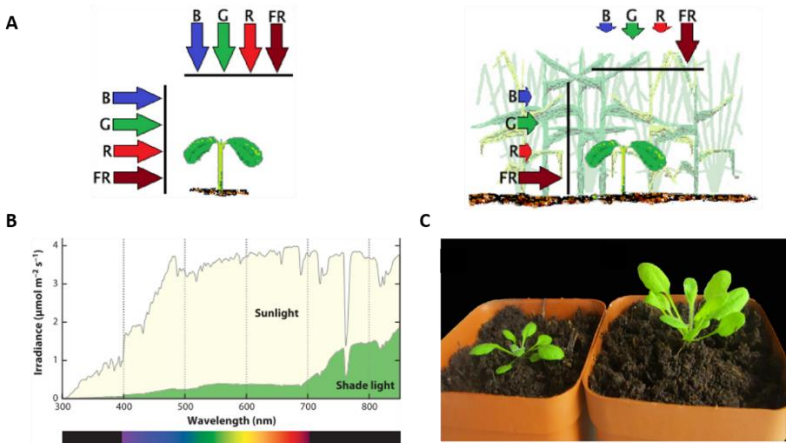

Figure 5. Shade light triggers Shade Avoidance Response (SAR). (A) Plant isolated from nearby vegetation (left) in contrast with plant shaded by an overhead canopy and surrounded neighbors (right) (Casal, 2012). (B) Spectral photon distribution of sunlight and shade light (Casal, 2013). (C) Phenotype of *Arabidopsis* plants grown under low (right) or high (left) red: far-red light (R:FR) ratio (Wang et al., 2020).

1.3.2 Signal transduction

The perception of the spectral differences, in specific circumstances results in SAR, firstly initiated by the excitation of specialized photoreceptors containing, at least one, nonprotein component known as chromophore. Chromophores are responsible for the photon absorption, eventually resulting in photoreceptors' conformational changes and the subsequent initiation of a signal cascade, known as light signaling. Higher plants have at least five types of sensory photoreceptors which allow the precise monitoring of light from UV-B to the near infrared (far-red). Specifically, red (R) and far-red (FR) light is sensed by the phytochromes (phyA–phyE in Arabidopsis), UV-A/blue light is sensed by cryptochromes, phototropins, and members of the Zeitlupe family (cry1, cry2, phot1, phot2, ZTL, FKF1, and LKP2 in *Arabidopsis*) (Kami et al., 2010; Heijde & Ulm, 2012), while recently a UV-B photoreceptor, called UV RESISTANCE LOCUS 8 (UVR8), was discovered (Rizzini et al., 2011).

While the sensory photoreceptors involved in perceiving differences between full light and shade light include phytochromes, cryptochromes, phototropins, UVR8 (Casal, 2013), phyB seems to exhibit a central role in SAS. Phytochromes exist in two photoconvertible forms, an inactive R-absorbing Pr form and an active FR-absorbing Pfr form. Under high R:FR (i.e., low vegetation density) the photoequilibrium is displaced toward the active Pfr form and the SAS is suppressed. On the contrary, under low R:FR the photoequilibrium is displaced towards the inactive Pr form and the SAS is induced (H. Smith & Whitelam, 1997; Harry Smith, 1982; Casal, 2012)

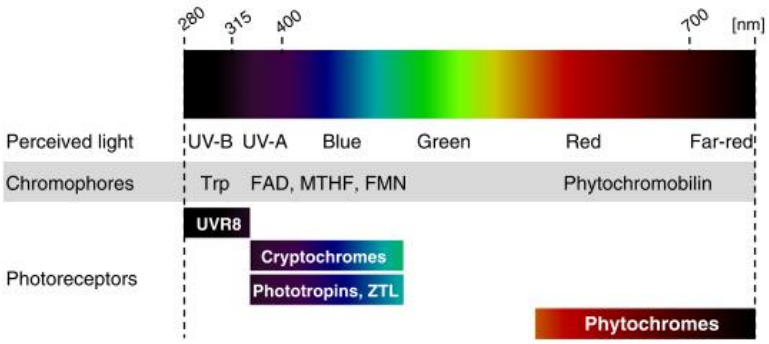

Figure 6. Photoreceptor-mediated light perception, from UV-B to infrared light, in higher plants (Heijde & Ulm, 2012)

Once activated the PHYB- Pfr is translocated into the nucleus where it interacts with a family of bHLH transcription factors, the PHYTOCHROME INTERACTING FACTORS (PIF). This interaction firstly results in blocking DNA-binding capacity of several PIFs, and secondly PIFs phosphorylation, subsequent ubiquitination and finally its degradation by the proteasome (Legris et al., 2019; Leivar et al., 2012). In low R:FR environments PHYB inactivation and thus stabilization of PIFs (i.e. PIF4, 5 and 7) triggers the expression of growth-promoting genes, mainly related to auxin biosynthesis (de Wit et al., 2016; C.Pantazopoulou, 2017). When grown in low R:FR, loss-of-function mutations in *TAA1* (TRYPTOPHAN AMINOTRANSFERASE OF ARABIDOPSIS, converts tryptophan into indole-3-pyruvate) or *PIF7* do not upregulate auxin levels and therefore do not exhibit SAR (L. Li et al., 2012).

Alongside decreases in R:FR ratio, shaded plants also perceive a reduction of ultraviolet-A (UVA) and blue light (B) and also an enrichment of green light (Casal, 2012). Low Blue Light (LBL) can also mediate shade avoidance response, mainly through CRY1 and CRY2 activation. Pedmale et al.(2016) showed that PIF4 and PIF5 act downstream of CRYs to mediate LBL-hypocotyl elongation. Specifically, CRY1 and CRY2 physically interacts with PIF4 and PIF5 but in distinct region comparatively to PHYB. Thus, they proposed a cross-talk between low R:FR and LBL signaling in shade avoidance (Pedmale et al., 2016). Additionally, similar to PHYA and PHYB active forms, CRYs, have been shown to bind SUPPRESSOR OF PHYA-105 (SPA) proteins and inhibit their interaction with CONSTITUTIVELY PHOTOMORPHOGENIC 1 (COP1) (Lian et al., 2011; Sheerin et al., 2015). COP1/SPA1 consists an E3 ubiquitin ligase complex degradating negative regulators of PIF activity such as HY5, HYH and HFR1 (Toledo-Ortiz et al., 2014).

Together all these data indicate CRYs contribution in SAR through LBL perception in shady environments.

Regarding the role of phototropins in blue light-controlled-shade avoidance response, this is, as yet, less studied. However, as phototropism is part of shade avoidance responses (Casal, 2012), phototropins (the principal photoreceptors controling this response) seems to be essential for SAR. Moreover, recently, a cross-talk between PHYB and PHOT1 in regulating phototropism in photoautotrophic seedlings was shown (Figure 7A) (Goyal et al., 2016a). Specifically, phyB seems to be a strong inhibitor of phototropism, particularly in high R:FR environments, by suppressing PIF4/5/7 and thus the expression of auxin-related genes and particularly *YUCCA* gene family. Therefore, in shady environments, where phyB exists in the Pfr inactivated form, PIF4/5/7 promote phototropism by YUC-mediated auxin production, which is probably important for the establishment of an auxin gradient between illuminated and shaded side. Additionally, a recent study suggest that phototropin is partly involved in typical shade avoidance response, such as promotion of stem elongation, plant flowering and leaf expansion, in association with low phytochrome activity (Kong & Zheng, 2020).

Finally, UVR8 photoreceptor, responsible for UV-B radiation perception, has recently reported to strongly repress SAR (Hayes et al., 2014). Following canopy closure, apart from R:FR, reductions in blue light intensities and UV-B signals true shade (Fraser et al., 2016; Sharma et al., 2019). In *Arabidopsis* seedlings grown under artificial light, moderate levels of supplemental UV-B can strongly suppress hypocotyl elongation responses to low R : FR ratio (Hayes et al., 2014). The suggested molecular mechanism for this response is based on UVR8-COP1/SPA1 interaction. More specifically, UV-B absorption monomerize the dimeric UVR8 forms, resulting in interaction of UVR8 with COP1/SPA1 complex and subsequent promotion of HY5 and HYH and PIF inactivation (Jenkins, 2017). This suggestion, is further supported with a recent study indicating that activation of the UVR8 promotes rapid PIF5 degradation via the ubiquitin-proteasome system (Sharma et al., 2019).

All the above-mentioned molecular mechanisms reveal a complex SAR signaling network involving multiple photoreceptors and modules (Figure 7B). Furthermore, PIFs seem to play a key-role in this network, whereas auxin biosynthesis and regulation are essential for the physiological and morphological changes underlying SAR.

Besides auxin, other hormones such as gibberellins (GA), brassinosteroids (BR) and ethylene also induce SAR, however the molecular mechanism linking hormones to shade avoidance is beyond the scope of this thesis. Briefly, ethylene is required for shade-induced petiole elongation, while auxin, GA and BR are involved in shade-regulated stem growth. Moreover, salicylic acid (SA) and jasmonic acid (JA) are repressed in low R:FR light conditions leading to decreased plant defense in shady environments, while strigolactone (SL) and abscisic acid (ABA) suppress branching (Figure 7C) (reviewed in: C. Yang & Li, 2017).

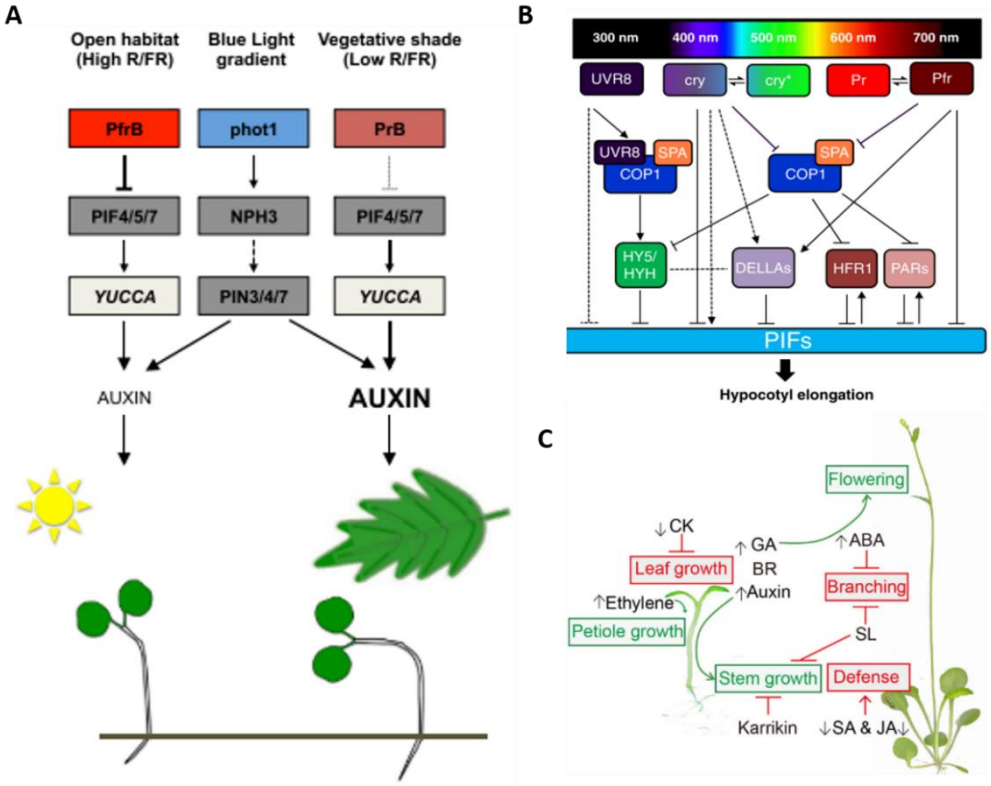

Figure 7. SAR: Photoreceptors, hormones and signal transduction. (A) Schematic representation of the crosstalk between Phot1 and PHYB in SAR-induced phototropism response (Goyal et al., 2016a). (B) Signal network involving multiple photoreceptors and the dominant role of PIFs in SAR (Fraser et al., 2016). (C) Hormonal regulation in shade avoidance (C. Yang & Li, 2017)

1.4 Phototropins: Blue light photoreceptors regulating multiple physiological responses

1.4.1 Structure and biological function

As briefly mentioned in the 1.3.2 section, phototropins are blue (390–500 nm) and ultraviolet-A (UV-A; 320–390 nm) photoreceptors, known principally, for their central role in phototropism response (Figure 8C)A) . Higher plants have two different phototropins, PHOT1 and PHOT2, while there have been duplication events in these genes, but only in some species (F. W. Li et al., 2015).

PHOT1 and PHOT2 regulate many physiological activities and seem to be functionally redundant (Figure 8C). Specifically, genetic analysis in *Arabidopsis* has shown that PHOT1 and PHOT2 overlap in function to regulate hypocotyl and root phototropism (Sakai et al., 2001), chloroplast accumulation movement (Kagawa et al., 2001), stomatal opening (Kinoshita et al., 2001), leaf positioning and leaf flattening (S. I. Inoue et al., 2008). However, depending on light intensity, some of the physiological responses seem to be activated by only one of the PHOTs . Thus, even though both PHOT1 and PHOT2 regulate hypocotyl phototropism in *Arabidopsis* in response to high intensities of unilateral blue light (> 1µmol m^{-2} s^{-1}), only PHOT1 mediates this response under low light (John M. Christie, 2007). Moreover, regarding the chloroplast accumulation movement to the upper cell surface, PHOT1 is more sensitive than PHOT2. In contrast, when higher plants sense high light intensity, chloroplast move away from

the side of irradiation to prevent photodamage of the photosynthetic apparatus in excess light (avoidance movement of chloroplast). This physiological response is only mediated by PHOT2, indicating that PHOTs can have unique roles. This is also the case for the hypocotyl growth inhibition mediated by solely PHOT1 upon blue light irradiation in etiolated seedlings (Kevin M. Folta et al., 2003). However, both PHOT1 and PHOT2 induce an increase in cytosolic [Ca^{2+}], which is a prerequisite for the hypocotyl inhibition mediated by PHOT1 (Harada & Shimazaki, 2007). Additionally, PHOT1 seems to be responsible for BL-mediated mRNA destabilization, even if it lacks an RNA binding capacity itself (Kevin M. Folta & Kaufman, 2003; Reichel et al., 2016).

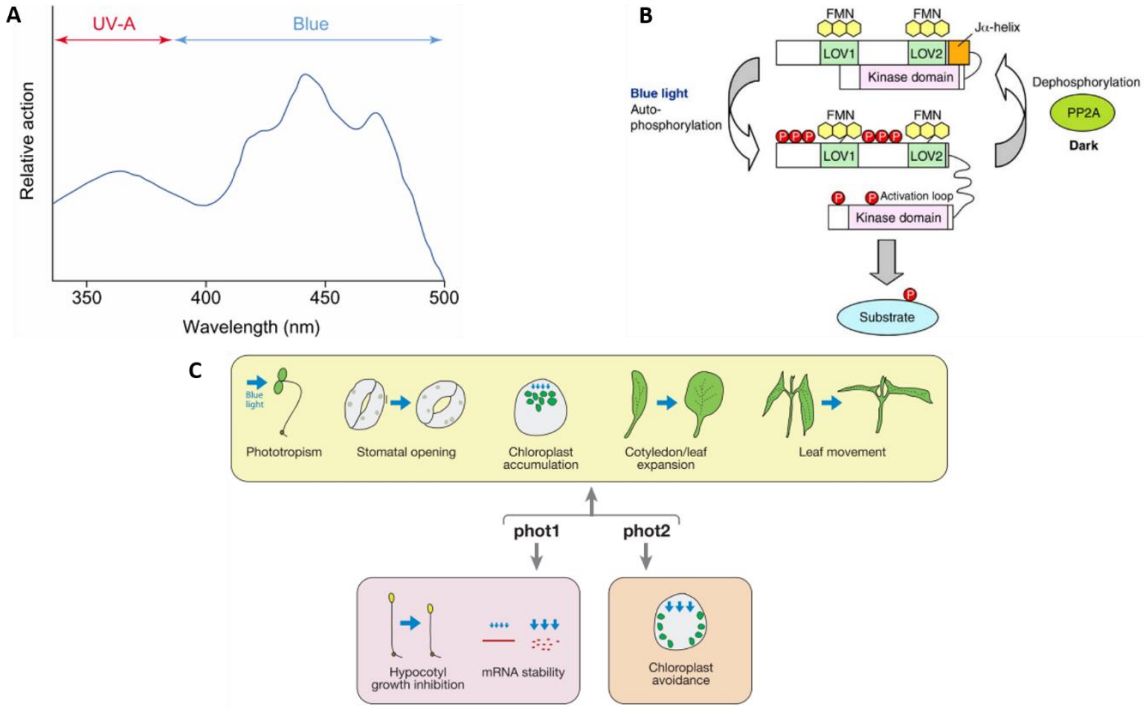

Figure 8. (A) Action spectrum typically observed for phototropin- mediated responses (Briggs & Christie, 2002) (B) A hypothetical model for the activation of phototropin molecules by blue light (S. ichiro Inoue et al., 2010) (C) Diagram illustrating the range of phototropin-induced responses in higher plants (John M. Christie, 2007)

1.4.2 Signal transduction: phototropism, leaf flattening and positioning

Here,I will describe succintly three relevant to my studies PHOT1-mediated responses, phototropism, leaf flattening and leaf positioning.

PHOTs status and localization is of great importance for the signal cascade to initiate. Xue et al. (2018) showed that PHOT1 exists mainly as monomers and dimers at the plasma membrane (PM) and that the dimerization rate increases upon blue light irradiation. The dimerization occurs within sterol-rich membrane microdomains (MM). Furthermore, upon blue light activation and consequently PHOT1 autophosphorylation, a portion of the pool of phot proteins becomes internalized (Figure 8B, Figure 9A) (Xue et al, 2018, Christie et al, 2018).

Furthermore, initial studies about the cellular and subcellular distribution of PHOT1 showed that upon BL stimulation, a fraction of PHOT1 is “released” from the plasma membrane to the

cytoplasm (Figure 9B) (Sakamoto & Briggs, 2002; Wan et al., 2008). However, even though the importance of the partial internalization of PHOT1 to cytosol, through clathrin-mediated endocytosis, has been marked especially for phototropism (Roberts et al., 2011), recent approaches aimed at tethering PHOT1 to the plasma membrane by myristoylation or farnesylation, found that incorporation of these modifications severely diminishes the light-induced internalization of PHOT1 without impacting its functionality in *Arabidopsis* (phototropism, petiole positioning, leaf flattening and chloroplast accumulation movement) (Preuten et al., 2015) (reviewed in: Liscum, 2016). Hence, the role of membrane-binding and detachment of PHOT1 is unknown.

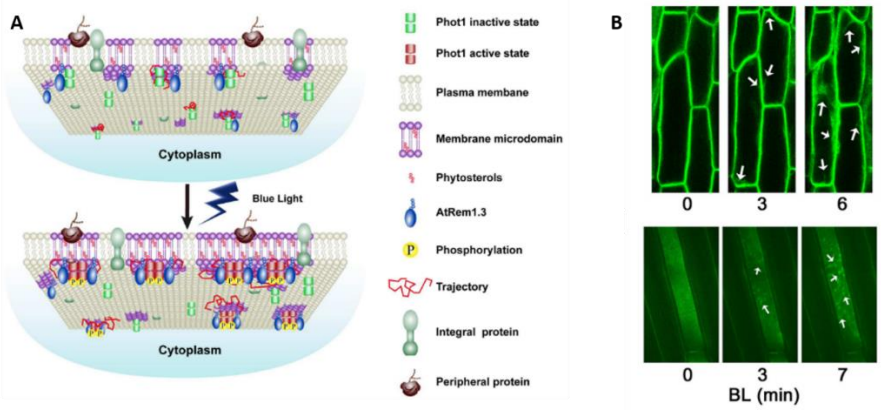

Figure 9. Initial signaling upon BL irradiation. (A) Phot-1 dimerization and autophosphorylation within membrane microdomains upon BL irradiation (Xue et al., 2018b). (B) phot-1-GFP punctate aggregation and formation of mosaics (arrows) after BL exposure. Confocal microscopy of cortical cells within the elongation zone just below the apical hook of etiolated seedling (reviewed in: Liscum, 2016)

Phototropism:

Upon unilateral irradiation, a light gradient is established across the stem, which creates a photoreceptor activation gradient between the irradiated and the shaded side. The early signaling events, after PHOT1 autophosphorylation are firstly characterized by the de-phosphorylation of the NON-PHOTOTROPIC HYPOCOTYL 3 (NPH3). In darkness, NPH3 is phosphorylated and localized to plasma membrane, interacting with the N-terminal portion of PHOT1 through its C-terminal region (Motchoulski & Liscum, 1999; Pedmale & Liscum, 2007; Haga et al., 2015). Immediately after irradiation (within 5 min), NPH3 is de-phosphorylated in a PHOT1 -dependent manner, its interaction with PHOT1 is inhibited and cytosolic aggregates form (Haga et al., 2015). The phosphorylation state of NPH3 changes again either in darkness or after long periods of irradiation leading to its relocation to the PM (Figure 10) (Haga et al., 2015; Christie et al., 2018; Legris & Boccaccini, 2020). However, the kinase(s) and phosphatase(s) responsible for this turnover remain to be identified (Haga et al., 2015; Sullivan et al., 2019a).

Recent findings, suggest that ROOT PHOTOTROPISM2 (RPT2) proteins accumulate following both R and BL irradiation and suppress PHOT1 activity through binding to the LOV1 domain (Kimura et al., 2020). Therefore, RPT2 indirectly suppress the NPH3 dephosphorylation and

aggregation, leading to an alleviated gradient of NPH3 across the irradiated and shaded hypocotyl sides. The NPH3 gradient formation seems however, necessary to drive hypocotyl phototropism (John M. Christie & Murphy, 2013; Sullivan et al., 2019a). Together all these data might suggest that RPT2 acts as a molecular rheostat that maintains a moderate activation of PHOT1 (Kimura et al., 2020), which is actually necessary for phototropism regulation, especially autotropism (the phenomenon of the organ straightening after bending). Furthermore, besides RPT2-dependent regulation of PHOT1 activity, previous data suggest that NPH3 display a similar role through its interaction with CULLIN3 (CUL3), a component of CULLIN3-based E3 ubiquitin ligase complexes (CLR3). In high-intensity BL, PHOT1 is both mono/multi- and polyubiquitinated by $CRL3^{NPH3}$, with the latter event targeting PHOT1 for 26S proteasome-mediated degradation (Roberts et al., 2011).

Besides NPH3-RPT2 -like (NRL) family, also Phytochrome Substrate Kinase family (PKS 1-4) is known to be involved in PHOT-mediated signalling pathway. Especially for phototropism, PKS4 is a substrate of PHOT1 kinase activity (Demarsy et al., 2012), as it seems to enhance phototropism in low BL, while inhibiting phototropism in high blue light following PHOT1-mediated phosphorylation (Schumacher et al., 2018).

Another phosphorylation substrate of PHOT1 is ABCB19 (J M Christie et al., 2011), a transmembrane auxin efflux carrier belonging to ABCB (for ATP Binding Cassette B) family. As *abcb19* mutants have exaggerated phototropism, it seems that this phosphorylation is not required to promote hypocotyl bending but rather to inhibit it (J M Christie et al., 2011).

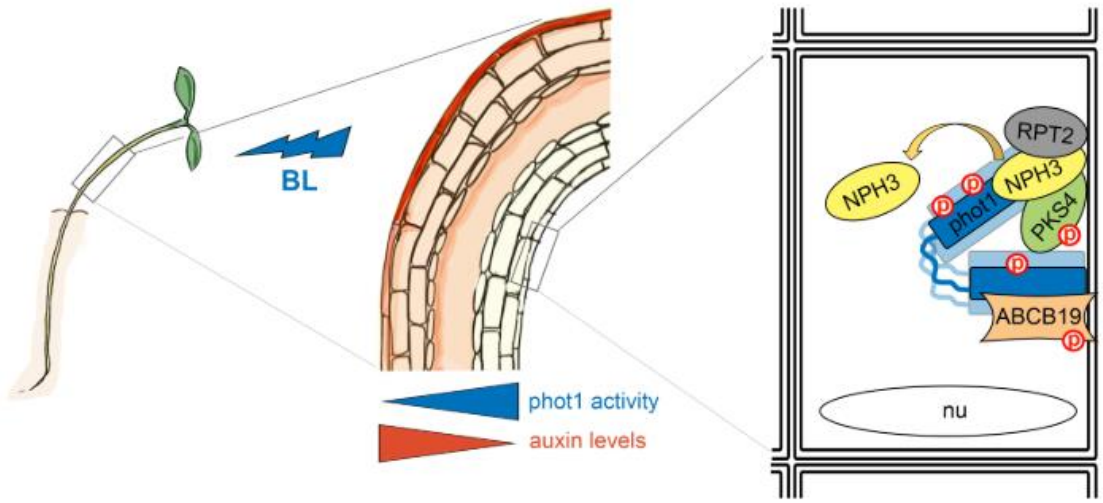

Figure 10. Hypocotyl curvature mediated by phot1. n Arabidopsis young seedlings, unilateral B irradiation drives hypocotyl curvature, which is the result of an increase in cell elongation in the shaded part of the hypocotyl compared to the lit side. This asymmetrical growth is accomplished by differential auxin distribution and phot1 activity across the hypocotyl. In blue light-irradiated cells, phot1 is activated and it starts a cascade of molecular events, which includes: NPH3 de-phosphorylation and internalization, phosphorylation of PKS4 and ABCB19 (Legris & Boccaccini, 2020)

Finally, the signal cascade leading to auxin gradient across the irradiated and shaded hypocotyl sides is essential for hypocotyl curvature (Figure 10). Besides ABCB19 direct involvement in PHOT1 signal transduction, the -PIN-FORMED efflux carriers (PIN1-4, PIN7 in

Arabidopsis) are also implicated in establishing this auxin gradient (Fankhauser & Christie, 2015; Liscum et al., 2014). Specifically, under conditions of darkness, PIN3 proteins are expressed in the hypocotyl endodermis, showing an apolar localization in endodermal cells. However, under unilateral white light irradiation (2 μmol m^{-2} s^{-1}), the PIN3 protein levels were found to be greatly decreased in the outer lateral side of the endodermal cells on the irradiated hypocotyl side in a PHOT1-dependent manner (Ding et al., 2011). Furthermore, the alteration of PIN3 distribution is also correlated with the auxin distribution pattern. This result, in combination with the decrease in the phototropic curvature of etiolated *pin3* mutated etiolated seedling, underline the main idea behind phototropic response: asymmetric auxin distribution upon unilateral irradiation results in an increase in elongation at the shaded side combined with a decrease in elongation at the irradiated side (Fankhauser & Christie, 2015).

For the scope of this study, the last worth-mentioning molecular alteration necessary for phototropism to happen, is microtubule reorientation. Microtubules control the differential growth response that underlies tropic responses in plants, including phototropism and gravitropism (Bisgrove, 2008). Sullivan et al., treated etiolated transgenic PHOT1-GFP *Arabidopsis* lines with oryzalin and they observed partial receptor internalization from the plasma membrane to cytoplasm, while the phototropic response of the treated samples was impaired. One explanation, came from Lindeboom et al. (2013), who showed that in PHOT1-stimulated microtubule reorientation (from transverse to longitudinal) katanin is required for hypocotyl curvature (Figure 11). Hence, phototropic impairment following oryzalin treatment is probably a result of microtubule depolymerization rather than an increase in PHOT1 internalization. In contrast, a new study indicates that the motor proteins myosins XIf and XIk are responsible for maintaining a balance between organ bending and straightening. Specifically, *myosin xif-1 xik-2* (loss of function mutants) hypocotyls exhibit enhanced bending in response to unilateral blue light irradiation (Okamoto et al., 2015)

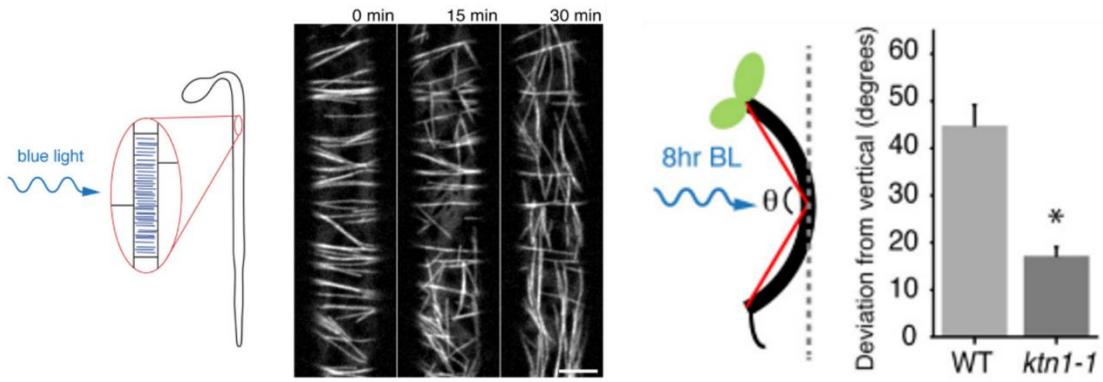

Figure 11. (Left): Microtubule reorientation (transverse to longitudinal) induced by blue light and mediated by katanin in a phot-dependent manner (Right): Plants deficient in Katanin1 (*ktn1-1* mutants) exhibit reduced phototropic bending (Lindeboom et al., 2013)

<u>Leaf positioning and flattening</u>

Although the molecular mechanism for the phot-mediated phototropism has been widely investigated, other PHOT-regulated physiological responses, such as leaf positioning and flattening, have attracted minor attention.

Leaf positioning, characterizing both the straight and upward growth of petioles, is induced by BL and it is mediated by PHOT1-signal transduction in low blue light, while in high intensities PHOT1 and PHOT2 act redundantly to mediate leaf positioning. Till today, NPH3, RPT2 and PHYTOCHROME KINASE SUBSTRATE 1-2 (PKS1, PKS2) have been implicated to this response, acting downstream of PHOTs (S. I. Inoue et al., 2008; de Carbonnel et al., 2010; Harada et al., 2013)(Harada et al., 2013; S. I. Inoue et al., 2008). Recent studies have also implicated ABCB19 in leaf positioning response, explaining at the same time, the changes in overall auxin levels, necessary for the displayed upright petiole angle. Specifically, low-fluence BL activates PHOT1, which phosphorylates to inactivate ABCB19, resulting in reduced long-distance auxin transport and increased auxin in the petioles. This accumulation finally results in PIN-directed transport to mediate leaf positioning (Jenness et al., 2020)

Regarding phot-mediated leaf flattening, similar components to leaf positioning seems to be involved. Even under high PAR, *phot1 phot2* double mutants, display curled leaf morphology, indicating that phototropins, and mainly phot2, are responsible for plant growth even under high radiation intensities (de Carbonnel et al., 2010). In addition, NPH3 mediates flattening on a PHOT1-depentdent manner, only under low blue light conditions (S. I. Inoue et al., 2008), while PKS1, PKS2 and RPT2 are also important regulators of the response (de Carbonnel et al., 2010; Harada et al., 2013). ABCB19 does not display a clear role during leaf-flattening response, as the expected phenotype of totally flattened leaves in *abcb19* mutant is not observed (Jenness et al., 2020). Nevertheless, BL activation of PHOT1 enhances auxin accumulations in the leaf tip and along the leaf margins, resulting in leaf flattening (Jenness et al., 2020), while, generally, spatial auxin signaling attenuate adaxial-abaxial polarity, leading to leaf flattening (Guan et al., 2017).

1.5 Aim of the study

The aim of my thesis was to investigate the role of KISC in light signaling, approaching the hypothesis from different perspectives. Firstly, through confirming or rejecting the interaction of Kin7.3 with components related to light-signaling (PHOT1, FHY3) and secondly, through the phenotypical and physiological characterization of KISC-related-loss-of-function mutants in response to different light qualities (white, blue, red). Furthermore, I aimed to investigate the genetic relationship between KISC-related and photoreceptors-related genes in order to better understand the involvement of KISC in light-dependent pathways. Finally, given the functional redundancy among Kin7.1, Kin7.3 and Kin7.5, at least regarding microtubule stability and root growth (Moschou et al., 2016), I also aimed to examine whether this genetic correlation also applies to light-dependent phenotypes.

2 Materials and methods

2.1 Physiology

2.1.1 Plant Materials and Growth conditions

The following genotypes of *Arabidopsis thaliana* were used for physiological experiments: the wild type (Columbia-0), *k135*, *kin7.3 rsw4* (Moschou et al., 2016), *phot1-5*, *phot1-5 phot2-1*, *phyAphyB*, *pifq* (Christie et al., 2011). *nph3* (SALK_122544C) and *abcb19* (SALK_033455) were ordered form NASC. For

crosses, besides all the above-mentioned lines, PHOT1 :: PHOT1-GFP and 35S::RFP-Kin7.3-tail X 35S:Pin2-GFP in Col-0 background and *phot2-1*, also used. All *Arabidopsis thaliana* lines were grown in a photostable growth chamber (FITOCLIMA 1.200; Aralab) (22° C, 66 ± 1% rH, 16h photoperiod), either on vertical plates containing half strength Murashige and Skoog medium (Duchefa), supplemented with 1% (w/v) sucrose and 0.8% (w/v) plant agar, or in canna terra soil. Light emitting diodes (LED) produce a highly peaked output in Blue, Red or Far-Red, were incorporated in growth chamber and used for the different light conditions needed for physiological experiments.

2.1.2 Hypocotyl growth rate measurements

Hypocotyl growth rates were measured as described by Kevin M. Folta et al. (2003). Briefly, for each genotype used, sterilized seeds were planted onto Petri dishes and stratified for 48h. After stratification, seeds were given a 2h Red light (105 µmol m^{-2} s^{-1}) treatment at 22°C to induce uniform germination. Plates were then kept in absolute dark in a vertical position at 22°C for 3-4 days. Hypocotyls were checked for length and vertical orientation with safe green light- emitting diode source (570nm). For hypocotyl growth inhibition stimulation, seedlings were overhead irradiated using a blue light-emitting diode source (470nm; 42 µmol m^{-2} s^{-1}). To test growth rates in response to BL, images were captured using a digital camera (D3500; Nikon) at 10-min intervals for 80min in darkness then for 2.30h in blue-light illumination. The length of hypocotyls was measured using ImageJ software (National Institutes of Health) and hypocotyl growth rates (dLength/dTime) were calculated.

2.1.3 Induction of Phototropism and Measurement of Curvature

For phototropism experiments seedlings were grown on 0.8% agar plates containing 1/4 Murashige Skoog medium (pH 5.7) supplemented with 0.5% sucrose. After stratification plates were kept in darkness in a vertical position at 22°C for 3 days. Etiolated seedlings with hypocotyls of approximately 3-4mm were irradiated with a unilateral blue light-emitting diode source (470nm; 20µmol m^{-2} s^{-1}), for 8-11h at 22°C. Images were captured at 1h intervals and the phototropic curvature was estimated as "deviation from the vertical hypocotyl growth" as described by Christie et al., 2011 (Figure 16B).

2.1.4 Leaf-positioning experiments

Measurement of petiole positioning was based on the protocol of Inoue et al. (2008a) with some modifications. For each genotype used, sterilized seeds were first planted onto agar Petri dishes and after stratification were grown under white light (150µmol m^{-2} s^{-1}) till reaching stage 1.02 (Boyes et al., 2001). Then, de-etiolated seedlings were transplanted into soil and transferred either under overhead white (150 µmol m^{-2} s^{-1}) or red (105 µmol m^{-2} s^{-1}) light for 4 more days until first true leaves were fully developed (stage 1.04; Boyes et al., 2001). Plants were exposed to red light and then transferred to overhead blue light (42 µmol m^{-2} s^{-1}) and they kept growing for 4 more days. Petiole angles were measured for plants grew under red or white light for 11 days and also for plants grew under red + blue and white light for 15 days. Measurements indicate the angle shaped by the median line of first true leaves and each petiole, subtracted by 90° in order to obtain an angle of petioles relative to horizontal axis (Figure 17A).

2.1.5 Leaf- flattening experiment

Leaf flattening was quantified as described by Jenness et al. (2020) with some modifications. Briefly, 7 days old de-etiolated plants grew on agar plates under white light (150 µmol m^{-2} s^{-1}) were transplanted into soil and transferred either to white (150 µmol m^{-2} s^{-1}), red (105 µmol m^{-2} s^{-1}) or blue (42 µmol m^{-2} s^{-1}) light. The fifth youngest rosette leaf from 25 days old plants was used for the measurements. Specifically, following removal, the adaxial side was imaged. Then, the leaves were manually uncurled and re-imaged. Both curled and uncurled leaf areas were measured using ImageJ software. Leaf flattening index was then calculated by dividing the curled with the uncurled leaf area.

2.2 Preparation of Agrobacterium strains

2.2.1 TAP plasmid material

TAP-constructs for genes corresponding to proteins emerged from Kin7.3 interactome were ordered from ABRC: At3g22845 (DKLAT3G22845), At5g48870 (DKLAT5G48870.1), At1g65700

(DKLAT1G65700.1), At3g63460 (DKLAT3G63460), At1g49750.1 (DKLAT1G49750), At3g20820 (DKLAT3G20820), At1g67680 (DKLAT1G67680), At5g21274.1 (DKLAT5G21274), At4g17520 (DKLAT4G17520.1), At4g16830 (DKLAT4G16830), At3g15010 (DKLAT3G15010), At5g15750.1 (DKLAT5G15750), At4g33050.2 (DKLAT4G33050). For FHY3 (At3g22170.1), CRCK2 (At4g00330.1) and PHOT1 (AT3G45780.1), DKLAT3G22170, DKLAT4G00330 and DKLAT3G45780 were used respectively as stock numbers for the order. All bacteria (strain: DH10B) transformed with the plasmids mentioned, were sent as stab LB agar cultures.

2.2.2 TAP plasmid isolation using alkaline lysis

An amount of liquid bacteria culture was centrifuged at 11.000xg for 30 seconds. The pellet was resuspended in resuspention buffer (50mM glucose, 25mM Tris-HCL pH 8.0, 10m M Na_2EDTA, 100mg/ml RNAse A), lysed in lysis buffer (0,2M NaOH, 1% SDS) and neutralized in neutralization buffer (3M NaOAc pH 4.8). After centrifugation at 12.600xg for 5 minutes, pure ethanol 100% was added to the supernatant and the tubes were centrifuged at 12.600xg for 10-20 minutes at 4oC. The resulting pellet was washed with 70% (v/v) ethanol and the tubes were centrifuged at 12.600xg for 5 min. After air-drying, the resulting pellet was dissolved in ddH_2O. All plasmids were then checked through digestion with suitable restriction enzymes and DNA Agarose Gel Electrophoresis.

2.2.3 Agrobacterium-mediated transformation

In order to finally proceed with the transient expression of the TAP-fused genes in *N. benthamiana*, TAP-constructs were used to transform Agrobacterium Gv3101 strain. Gv3101 competent cells were thawed on ice and isolated plasmid was added. The mixture was transferred to liquid nitrogen for 2 sec to induce cold shock. After incubation for 30min at 37°C water bath (heat shock), YEP (10g L^{-1} yeast extract, 10g L^{-1} peptone, 5g L^{-1} NaCl) medium was added to the tubes. After outgrowth for 3h at 28°C with agitation, transformants were selected on YEP agar plates containing spectinomycin (50 ug/ml; TAP-selection marker), gentamycin (10 ug/ml) and rifampicin (100 ug/ml). The cells were incubated for 2-3 days at 28°C and single colonies were selected.

2.3 Agroinfiltration-Transient expression in *N. benthamiana*

Single colonies for Agrobacteria, containing separately p19 (rif^R, $spec^R$), YFP-Kin7.3-Tail (in pGWB542, rif^R, $spec^R$, $gent^R$), eGFP (in p7FWGF2, rif^R, $spec^R$) and TAP-constructs (LIC6, rif^R, $spec^R$; pYL436, rif^R, $spec^R$, $gent^R$) were inoculated into YEP medium supplemented with the appropriate antibiotic (Figure S 3). The cultures were incubated for 16-20h in the dark at 28°C. Agrobacterium cells were pelleted by centrifugation at 2800xg for 10min at 4oC, and resuspended in 2xV MES buffer (MES 10mM, $MgCl_2$ 10mM, Acetosyringone 200µM). The cells were centrifuged in the same conditions after incubating in the dark shaking for 2-3h at 28°C. The pellet was re-diluted in 2XV MgCl2 10mM and centrifuged again. 1ml of MES 10mM, $MgCl_2$ 10mM solution was used to dissolve the pellet and after OD^{600} measurement, the optical density was adjusted to a final 0.4 OD. Each one of the Agrobacterium strains containing YFP-Kin7.3t, eGFP and TAP-construct were mixed together with p19 Agrobacterium strain before infiltration in order to suppress gene silencing. Top leaves of 2-4 week old *N. benthamiana* plants were used for infiltration, excluding the youngest leaf. *Agrobacterium* suspension was infiltrated into the whole leaf area from a small cut in the lower epidermis, using a needless syringe. After agroinfiltration, the plants were kept in the growth chamber for 3 days before leaf harvesting.

2.4 Co-Immunoprecipitations

2.4.1 IgG-pull-downs.

Tissue from agroinfiltrated leaves was ground in liquid N_2, thawed in 3 volumes of extraction buffer (50 mM Tris–HCl pH 7.5, 150 mM NaCl, 10% glycerol, 0.5% Nonidet P-40, 1 mM DTT, and 100x complete protease inhibitor cocktail) and incubated on ice for 20 min, while vortexing every 5 min. The mix was centrifuged at 15.500 rpm for 15 min at 4°C, while the supernatant was filtered through miracloth. 50 µl of the filtered supernatant were kept as input. Extracts, were incubated with 25µL IgG washed beads for 2h at 4°C with gentle rotation. After centrifugation at 800g for 5min at 4°C, the IgG beads were recovered and washed 4 times with washing buffer (50 mM Tris–HCl pH 7.5, 150 mM NaCl, 10% glycerol, 0.5% Nonidet P-40, 1 mM DTT). For the elution of TAP-tagged proteins, 25 µl of beads were

resuspended in 4x laemmli buffer and after boiling for 5 min at 95°C, the mixture was centrifuged at 16,000 rpm for 5min at 4°C. For different elution methods, washed IgG beads were treated with 2µl PreScission protease (Sigma-Aldrich) diluted in 200µl washing buffer and incubated overnight at 4°C with gentle rotation. Alternatively, washed IgG beads were treated with 1:10 volumes of 0.1M Glycine-Cl (pH=2.8) and incubated at RT for 15min, vortexing every 5min. After centrifugation at 800g for 5min at 4°C, 50µl of supernatant, regardless of the elution method, was resuspended in 4x laemmli buffer and boiled for 5min at 95°C for protein denaturation. Protein levels were identified by SDS-PAGE followed by Western blot. Protein immunodetection on polyvinylidene difluoride (PVDF) membranes was performed using Clarity ECL Western Blotting Substrates kit (BIO-RAD) and Sapphire Biomolecular Imager (Azure Biosystems).

2.4.2 YFP/GFP-pull-down

Protein extraction was performed as described above (IgG-pull-down) with the exception of the extraction buffer composition (50 mM Tris–HCl pH 7.5, 150 mM NaCl, 10% glycerol, 0.1% Triton-X-100, 1 mM DTT, 1xPhosSTOP (Sigma-Aldrich), 1xMG132 (Sigma-Aldrich) and 25x complete protease inhibitor cocktail). Protein extracts were treated with 20µL GFP-Trap® Magnetic Agarose beads (slurry) and incubated for 2h at 4°C with gentle rotation. Beads were washed 5 times with washing buffer, using PureProteome™ Magnetic Stand (Sigma-Aldrich). Then, beads were eluted using 1:4 volumes of SDS Sample Loading Buffer (Laemmli).

3 Results

3.1 Validation of Kin7.3 interactions

3.1.1 Establishment of method

As mentioned above, PHOT1 was identified as a Kin7.3 interactor. The interactome of Kin7.3 was conducted using affinity purification combined with mass spectrometry analysis (AP/MS), and thus, further validation had to be done due to the false positive results of the technique (Bontinck et al., 2018; Titeca et al., 2019). Therefore, I used co-immunoprecipitation (Co-IP) technique in order to validate interactions. However, I firstly had to try, different pull-down approaches and different elution methods, in order to proceed with the most efficient one. For the establishment of the method I used different potential interactors of Kin7.3 (data not shown). The constructs I worked with were: the truncated version of Kin7.3 containing only the tail domain (Kin7.3t), cloned into pGWB542 binary vector (YFP-N-terminal fusions) and either the genomic, cDNA or coding sequence (CDS) of the potential interactors, cloned into TAP-tagged expression vectors (LIC6 or pYL436) (For the potential interactors used, see materials and methods and Figure S 2). TAP-tag is composed of the immunoglobulin-binding domain of protein A from Staphylococcus aureus (2xIgG-BD), a human rhinovirus 3C (3C) protease cleavage site, a six histidine repeat (6xHis) and nine myc epitopes (9xmyc), while it allows the tandem affinity purification (TAP) of protein complex (Rubio et al., 2005).

After having transiently co-expressed the YFP-Kin7.3t and the TAP-protein of interest in *N. benthamiana* leaves, I subsequently proceeded with total protein extraction. Then, I followed different Co-IP approaches. Firstly, I used IgG Sepharose beads (Sigma-Aldrich) for the pull-down, taking advantage of the 2xIgG-BD of the TAP-protein (CRCK2-TAP; calmodulin-binding receptor-like cytoplasmic kinase 2). For the elution, I used either 4 x SDS sample buffer (laemmli), 0.1 M Glycine-Cl (pH=2.7), or 3C protease (Prescission protease; Sigma-Aldrich).

Finally, TAP-tagged protein and YFP-Kin7.3t were detected through western blot using anti-myc and anti-GFP antibodies respectively (Figure 12A). However, even though elution with

Glycine-Cl and 3C protease worked, I chose to conduct reciprocal coIP, using anti-GFP/YFP magnetic agarose beads (ChromoTek GFP-Trap®),. This decision was based on the inherent properties of IgG beads to bind our antibodies, thereby, producing increased noise in my blots that masked YFP signals of the low expressed YFP-Kin7.3t. The reciprocal YFP-pull-down proved more efficient, as it resulted in a clear enrichment of the bait. Furthermore, I optimized the detergent used for the YFP-Kin7.3t; most efficient non-ionic detergent appeared to be Triton-X-100, compared to Tween-20 and Nonidet P-40, as resulted in a better solubilization (Figure 12B).

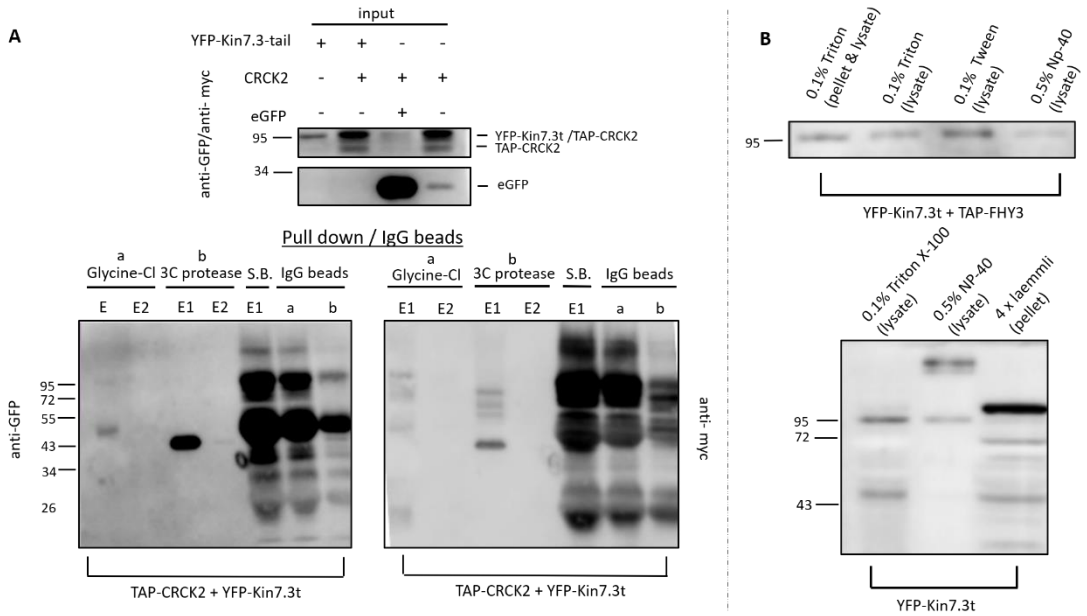

Figure 12. Refinement of the TAP-purification method for our proteins of interest. (A) Co-IP for TAP-CRCK2 and YFP-Kin7.3t. Lower YFP-Kin7.3 detection compared to CRCK2 (input) and different elution methods after IgG pull-down. Sample buffer (4x Laemmli); SB (B) Different detergent for protein extraction. 0.1% Triton-X-100 seems to better solubilize YFP-Kin7.3t

3.1.2 PHOT1 interacts with Kin7.3 tail domain

In order to investigate PHOT1 and Kin7.3 interaction I performed *Agrobacterium*-mediated transient expression of PHOT1-TAP and YFP-Kin7.3t in *N. benthamiana* leaves. Furthermore, free GFP (eGFP) was co-infiltrated together with PHOT1-TAP (negative control). Taking into consideration that PHOT1 exists in two different conformation states depending on the light quality, I investigated the possibility of Kin7.3 interacting with the active as well as the inactive PHOT1 form, using different light conditions. Thus, after agroinfiltration, *N. benthamiana* grew for 4 more days either with an overhead white light (150 µmol m^{-2} s^{-1}), under which PHOT1 is active or with Far-Red (FR) light (25 µmol m^{-2} s^{-1}), under which PHOT1 is inactive (Figure 6). Following protein extraction and Co-IP, it was shown that although Kin7.3t interacts both with the active and the inactive PHOT1 form, it may prefer the latter (Figure 13).

Furthermore, the immunoreactive YFP-Kin7.3t appears as two distinct migrating forms in white light, while in FR the faster migrating form is merely detected. As already mentioned,

PHOT1 has a C-terminal serine/threonine protein kinase domain (PKD). Upon blue light absorption the repression of PKD by the N-terminal photosensory domain is alleviated, leading to PHOT1 conformational change, its subsequent autophosphorylation and the initiation of a signal transduction. The active PKD domain can result in the phosphorylation of interacting components such as PKS4 (Demarsy et al., 2012). In contrast, NPH3, a central component in PHOT1 signal transduction, has been reported to be dephosphorylated upon blue light PHOT1-activation, in a PHOT1-dependent manner (Pedmale & Liscum, 2007b; Sullivan et al., 2019b). Thus, as PHOT1 interacts with Kin7.3 at least *in vitro*, I hypothesized that the distinct migrating forms observed, correspond to phosphorylated and dephosphorylated isoforms of Kin7.3t. In contrast, it would be also possible that the electrophoretic mobility shift could be due to partial proteolysis, or even due to a different post-translational modification (e.g. glycosylation).

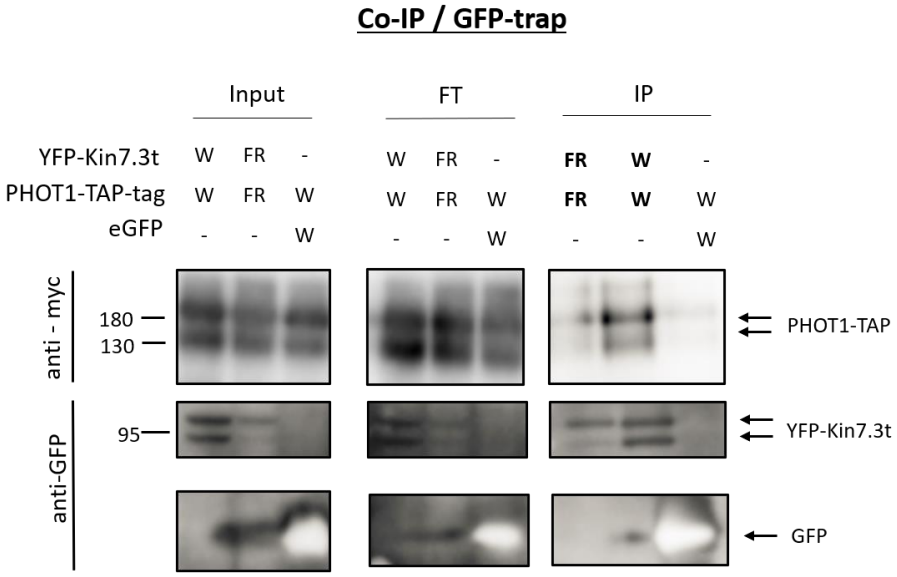

Figure 13. Kin7.3t interacts with PHOT1 both under WL and FR. Co-immunoprecipitation (IP) of TAP-fusions of PHOT1 with YFP-Kin7.3t in *N. benthamiana* leaves (4 days post infiltration). Membrane was probed with anti-myc and re-probed with anti-GFP.

In order to investigate this hypothesis, I conducted a preliminary experiment, using YFP-Kin7.3t agroinfiltrated in *N. benthamiana* leaves. The protein extracts were incubated for different time points either with phosphatase inhibitors (phosSTOP; Sigma-Aldrich) or with Alkaline Phosphatase, Calf Intestinal (CIP; NEB), in order to monitor a possible electrophoretic mobility shift in YFP-Kin7.3t, through western-blot. However, I could not reach a safe conclusion, mainly due to the absence of a positive control for the enzymatic activity of CIP (Figure S 4D).

Besides PHOT1-Kin7.3t, I also investigated FYH3-Kin7.3t interaction following the same steps, as described above. As shown in Figure 14, FHY3-TAP/Kin7.3t did not interact under the conditions used.

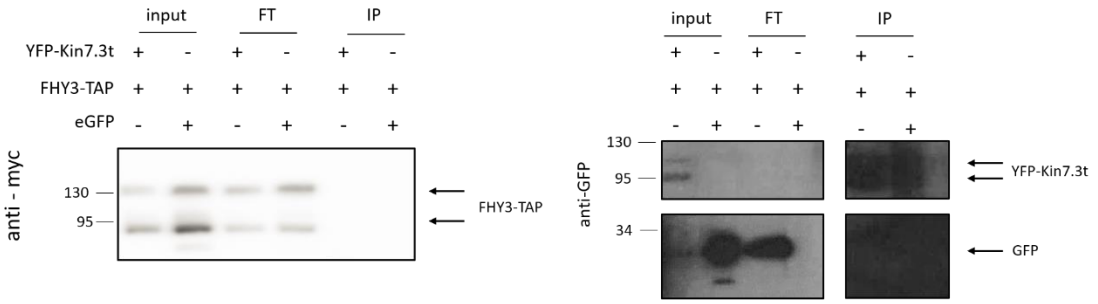

Figure 14. FHY3 does not interact with Kin7.3t under the the experimental conditions used. Co-immunoprecipitation (IP) of TAP-tagged versions of FHY3 with YFP-Kin7.3t expressed in *N. benthamiana* leaves (4 days post infiltration). Membrane was probed with anti-myc and re-probed with anti-GFP.

3.2 Kinesin7.3 clade is probably involved in hypocotyl growth inhibition upon BL irradiation

As Kin7.3 seems to interact with PHOT1, I further investigated its implication in PHOT1-dependent physiological responses. Due to the functionally redundant role of Kin7.1, Kin7.3 and Kin7.5 at least regarding microtubule stability and plant growth (Moschou et al., 2016), I investigated the phenotype of *k135* triple mutant which harbors T-DNA insertion either in the motor or the tail domain of Kinesins (Figure S 1B). Specifically, it has been reported that in etiolated seedlings, PHOT1 interferes with hypocotyl growth rate upon BL stimulation via increases in [Ca2+cyt](K. M. Folta & Spalding, 2001; Kevin M. Folta et al., 2003). Therefore, I measured the hypocotyl growth kinetics of etiolated seedlings Col-0, *phot1*, *phot1phot2*, and *k135*, for 80min (10min intervals) and then I exposed seedlings to continuous BL (42 µmol m^{-2} s^{-1}), measuring again the kinetic for 2.5 h (10min intervals). As shown in Figure 15, *phot1-5 phot1-2* cannot sense BL and thus it exhibits steady hypocotyl growth rate with respect to Col-0. Even though the resulting measurements are not clearly consistent with previous reports indicating great differences between Col-0 and *phot1-5*, *phot1-5 phot2-1*, it seems that *k135* hypocotyl growth pattern corresponds better to the one of *phot1-5*, giving a preliminary evidence for their synergistic action in hypocotyl growth inhibition (Figure 15).

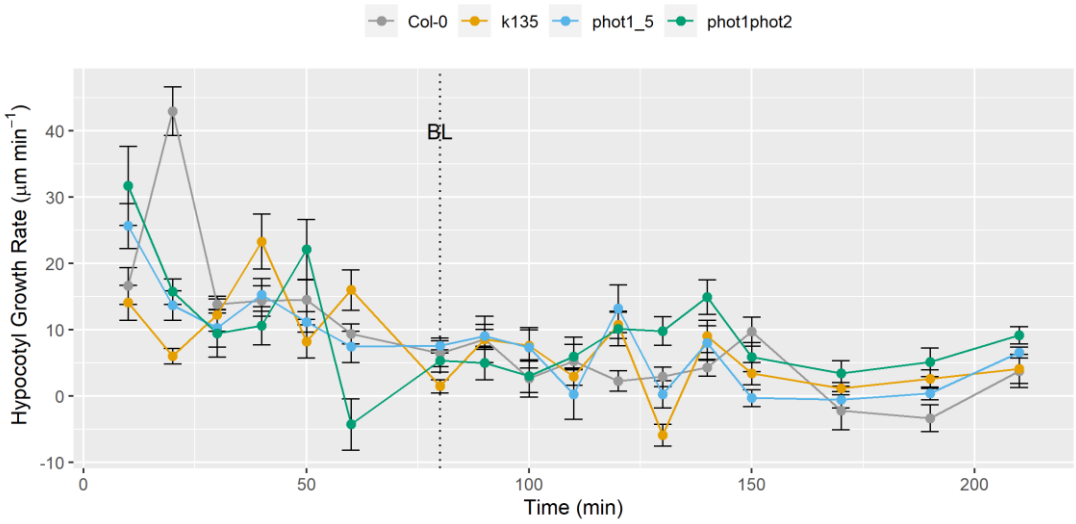

Figure 15. Kin7.3 clade seems to contribute to the phot1-mediated primary hypocotyl growth inhibition. Etiolated Col-0, *k135*, *phot1-5*, *phot1-5 phot2-1* seedlings grew vertically in agar plated for 3d in dark. The hypocotyl growth kinetic was measured for 80min and 2.5h in the dark and continuous BL (50 µmol m^{-2} s^{-1}) respectively. Data points represent the mean growth rate of at least 12 independent seedlings, and error bars represent SE/2. Statistics regarding population distribution were done using Shapiro-Wilk test and Q-Q (quantile-quantile) plots (Figure S 1C).

3.3 KISC is involved in autotropism response

The *phot1* loss of function mutant results in the incapability of the etiolated seedling to bend towards directional light in both low- and high-BL, while *phot2* is important for high BL intensities (reviewed in: Goyal et al., 2013; John M. Christie et al., 2018; Legris & Boccaccini, 2020). Furthermore, NPH3 appears to be a key component in this response, as *Arabidopsis* mutants lacking NPH3 fail to exhibit phototropism under a variety of different light conditions, both in etiolated and de-etiolated mutants (Motchoulski & Liscum, 1999; Fankhauser & Christie, 2015; Haga et al., 2015; Sullivan et al., 2019). In contrast, *abcb19* mutants show enhanced bending relative to wild type, which is evident as early as 2–4 h after exposure to directional low-BL (J M Christie et al., 2011). However, this pattern only refers to dark-acclimated *Arabidopsis* seedlings (de-etiolated seedlings subjected to 24-h period of dark acclimation prior to phototropism). Furthermore, in response to continuous low-intensity BL (absence of red-light pretreatment), a *phyA* and mostly *phyAphyB* double mutants show strong phototropic defects in etiolated seedlings, deteriorating in the absence of RL pretreatment (Parks et al., 1996). Recent studies indicate that phyA contributes to enhanced phototropism in etiolated seedlings, while phyB is a strong inhibitor of phototropism in photoautotrophic seedlings particularly in high R/FR environments, suggesting an antagonistic role between phyB and phototropins (Goyal et al., 2016b).

Taking into consideration the primary role of both PHOT1/2 in mediating phototropic response, as well as the contributions of PhyA/B, I investigated whether Kin7.3, as well as, Kin7.1 and Kin7.5, display a deviating phototropic pattern comparing, firstly, to wild type *A. thaliana* (Col-0). As I used different intensity of directional blue light in comparison with the literature (20 µmol m^{-2} s^{-1}) I firstly validated the setup of the experiment by using Col-0 as a positive control for phototropism, and *phot1-5*, *phot1-5 phot2-1*, *nph3*, *abcb19* mutants

(Figure 16A). Three-days old etiolated seedlings were subjected to 8h unilateral BL illumination, regarding Col-0, *k135*, *kin7.3rsw4*, *phot1*, *phot1-5 phot2-1*, and *phyAphyB* genotypes. Before stimulation of phototropic response, I irradiated the seedlings with overhead RL (110 µmol m^{-2} s^{-1}) for 15min, in exclude Phys functions in the phototropic responses. As shown in Figure 16B, the triple *k135* mutant display a hyberbending response in comparison to WT(Col-0), while *k7.3rsw4* exhibit the same deviation pattern, but interestingly, to a greater extent.

As I have not tested phototropic pattern of *k7.3rsw4 phot1* or *k135 phot1* I cannot conclude that Kin7.3-clade function is PHOT1-dependent. For instance, *Arabidopsis* mutants defective in the motor protein myosin XI (specifically XIf and XIk) or ACTIN8 exhibit hyperbending of stems in response to unilateral continuous BL photostimulation (Okamoto et al., 2015). Thus, considering the primary role of KISC in regulating microtubule stabilization, as well as the redundant role of Kin7.1, Kin7.3 and Kin7.5 regarding this response (Moschou et al., 2016), the resulting phototropic pattern observed in the relevant mutant lines, seems reasonable. Furthermore, I hypothesize that Kin7.3-clade, could contribute to the stem straightening (autotropism), a necessary response, which leads to the stop of bending in order for the plant to attain its desired position (Okamoto et al., 2015).

Regarding the more severe deviation from the vertical grwoth axis observed for *kin7.3rsw4*, this could relate to the *ESP* mutation (*rsw4*). However, this hypothesis needs to be confirmed using *rsw4* single mutant as control. Another explanation, in addition to the above-mentioned hypothesis, comes from the nature of *k135* triple mutation. Specifically, kin7.1 and kin7.5 mutants have T-DNA insertions in their motor domains and do not show transcription of the N-terminal region (Figure S 1B). In contrast, *kin7.3* allele can potentially produce a truncated version of Kin7.3 with a motor domain and a partial AtESP interaction domain (Kin7.3^{1-717}) that show weak binding to AtESP (Moschou et al., 2016). Thus, the milder phenotype of *k135* mutant, in comparison with the ones observed in *kin7.3rsw4*, could be attribute, to the partially activated KISC complex.

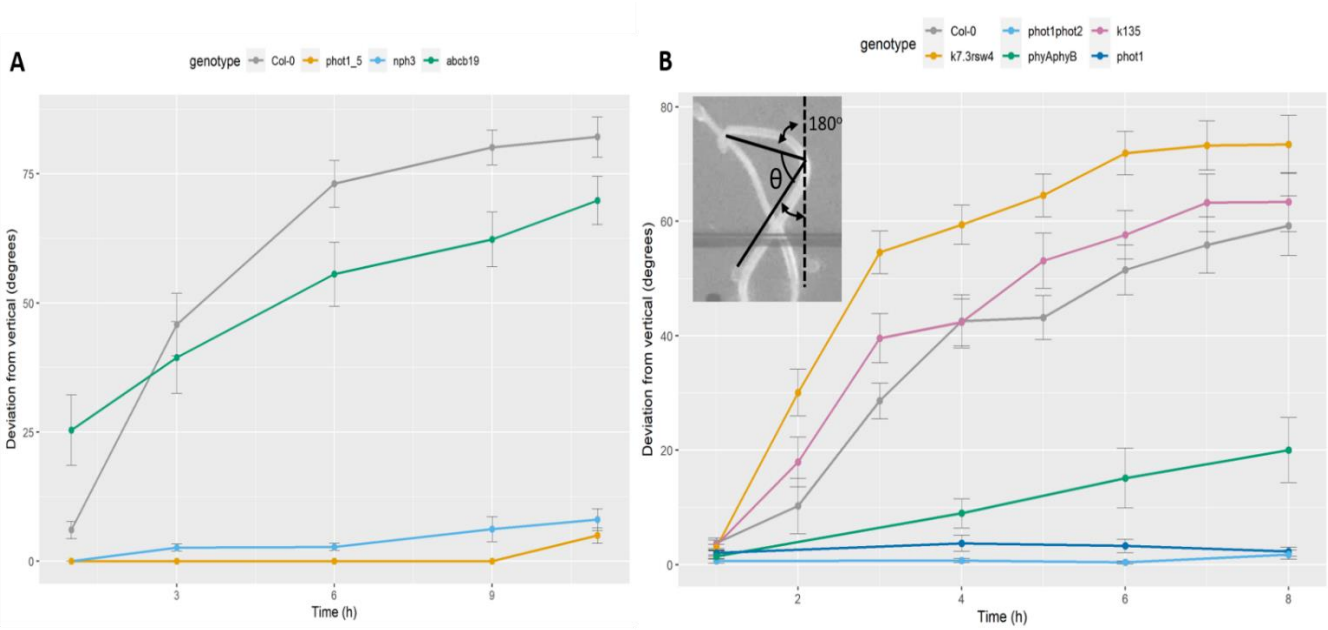

Figure 16. Phototropic response of various mutants involved in light perception/bending responses of the hypocotyl. (A). Refinement of method. Col-0, *phot1-5*, *nph3*, *abcb19*, were used in a pilot experiment. *phot1* and *nph3* display severe phototropic defects, while *abcb19* initially shows increased hypocotyl curvature, however, this phenotype dimishes with time. (B) Phototropic time course for wild-type (Col-0), *phot1–5*, *phot1phot2*, *k135*, *kin7.3rsw4* and *phyAphyB*. Hypocotyl deviation from the vertical axis as described previously (J M Christie et al., 2011). Results represent the mean ± SE, n ≥ 15.

3.4 KISC is involved in leaf positioning response

Hyponasty mainly refers to the upward leaf movement, observed in low R/FR and results from the differential petiole growth and elongation of stems and petioles. Thus, leaves occupy elevated position towards the more illuminated parts of the canopy. However, regarding the shade-induced hyponastic growth, besides phyA and phyB, also, Cry1 and Cry2 play a major role through low blue light perception (Millenaar et al., 2009). Even though PHOT were first reported not to regulate hyponasty response (Millenaar et al., 2009; Mullen et al., 2006), Inoue et al. (2008b), reported that when red light was at the same time supplemented with BL, the leaf surface was perpendicular to the light direction due to both the straight and upward growth of petioles, in contrast with the arched petioles observed in RL alone. They called the response "leaf positioning" and they showed that it is PHOT1-mediated in low BL and PHOT2-mediated in high BL intensities. Further studies demonstrated key roles for NPH3, RPT2 and ABCB19for the regulation of leaf positioning acting downstream of PHOTs (de Carbonnel et al., 2010; Harada et al., 2013; S. I. Inoue et al., 2008; Jenness et al., 2020). In conclusion, it seems that the upward petiole growth is regulated by a still poorly understood crosstalk among different photoreceptor-mediated pathways (phyA, phyB, cry1, cry2, phot1, phot2), acting also differently regarding the light intensities.

As already mentioned, *k135* and *k7.3* mutants seem to display a hyponastic phenotype at the almost fully developed rosette stage (Figure 4). While PHOTs have not been reported to regulate the response in this developmental stage, I firstly investigated the leaf positioning in either 1.02 or 1.04 stage (Boyes et al., 2001), when 2 or 4 true leaves have emerged, respectively. I used Col-0 (wild type) and *k135*, *k7.3rsw4*, *phot1-5*, *phot1-5 phot2-1*, *nph3*,

abcb19, *phyAphyB* and *pifq* mutant lines in order to monitor both the PHOTs- and PHYs-mediated response. The experimental setting was as follows. I grew plants on agar plates, in white light (150 µmol m^{-2} s^{-1}) for 7d to induce de-etiolation. De-etiolated plants had a pair of cotyledons and undeveloped first true leaves. I then transplanted the plants in soil and I transferred them either in overhead RL (105 µmol m^{-2} s^{-1}, 16h photoperiod) or WL (150 µmol m^{-2} s^{-1}, 16h photoperiod) and I kept them under the same conditions for 4 more days till the first true leaves were fully developed. Then I measured the petiole angle of the first true leaf in both conditions. As shown in Figure 17A, *phot1-5*, *phot1-5 phot2-1* and *nph3* display significantly reduced petiole angle in RL, in contrast to *k7.3rsw4*, *k135*, *abcb19*, *phyAphyB*, but also Col-0, in which a slight decrease is observed. The only exception comes from *pifq,* which, nevertheless, display constitutively photomorphogenic phenotype. *k7.3rsw4* phenotype resembles *abcb19* and *phyAphyB* : they display significantly greater leaf elevation compared to WT both in WL and RL.

In order to further examine the genetic relationship between the above-mentioned genotypes I proceeded with BL treatment. Specifically, I transferred the already exposed RL plants, to overhead high intensity BL (42 µmol m^{-2} s^{-1}, 16h photoperiod) for 4 more days in order to compare the leaf elevation between the R- and BL-exposed first true leaves among the different genotypes. In order to ensure that changes in petiole angle do not reflect different age between “red” and “red + blue” plants, I compared the petiole angle growing in WL either for 11days or 15days.

However, leaf elevation seems to be also age-dependent, as in all genotypes tested, first true leaves of 15 days old plants display decreased petiole angle comparing to the corresponding leaves of 11 days old plants (Figure 17; Figure 18). Thus, the direct comparison of leaf positioning between “red” and “red + blue” plants was not possible. However, in consistency with the literature, comparing the same-age “blue + red” and “white” light plants seems that in BL-sensing either from PHOTs or CRYs plays a major role in leaf positioning (Figure 18A). This can be clearly justified by the fact that “red + blue” (15 days old plants) WT and *pifq* display more increased petiole angles comparing with the ones grown in WL even for 11 days.

Furthermore, PHOT2 clearly contributes to this response as *phot1-5 phot2-1* is the only mutant line that continues to display statistically significant difference from the WT. Finally, the elevated petioles observed in “red” *k7.3rsw4* are probably due to a downstream signal initiated by the active Pfr form of phyB, as the blue light supplementation almost rescued the phenotype of both “red” *k7.3rsw4* and *phot1*. However, as k7.3 interacts with phot1, a crosstalk between phyB and phot1 in regulating leaf positioning cannot be refuted. In any case, additional experiments need to be done in order to examine the light signaling for leaf positioning response, as well as the involvement of Kin7.3 and KISC in the pathway, which could also be light-independent, as hyponasty results as a response in different kinds of abiotic stress.

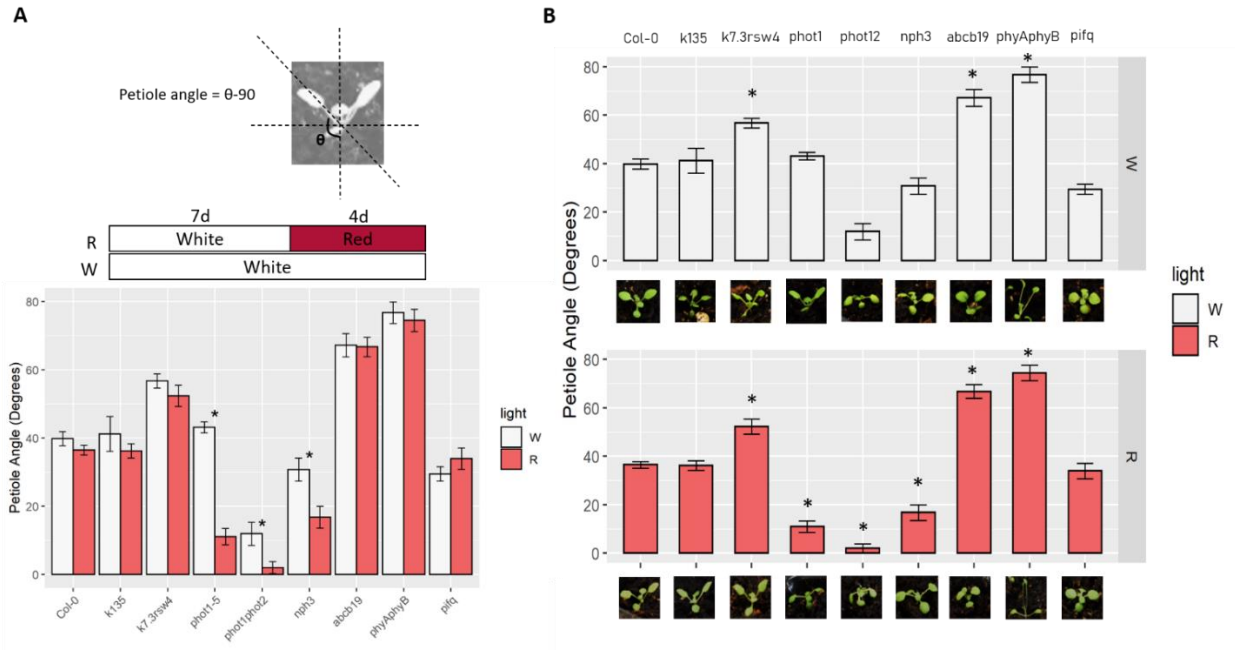

Figure 17. Involvement of KISC in leaf positioning (a). Leaf positioning was determined after light treatments by measuring the hypocotyl-petiole angle; 90º was subtracted to provide an indication of petiole position relative to horizontal axis (inset in A). When plants reached stage 1.02, they were transferred to soil either to 105 µmol m^{-2} s^{-1} red light (R) or 150 µmol m^{-2} s^{-1} white light (W) and allowed to grow for 4d. (A) grouping according to genotype (B) grouping according to light. Data shown represent means ± SE (10 ≥ n ≥ 15). Asterisks indicate statistical difference by one-way ANOVA followed by Tukey's HSD (P < 0.05).

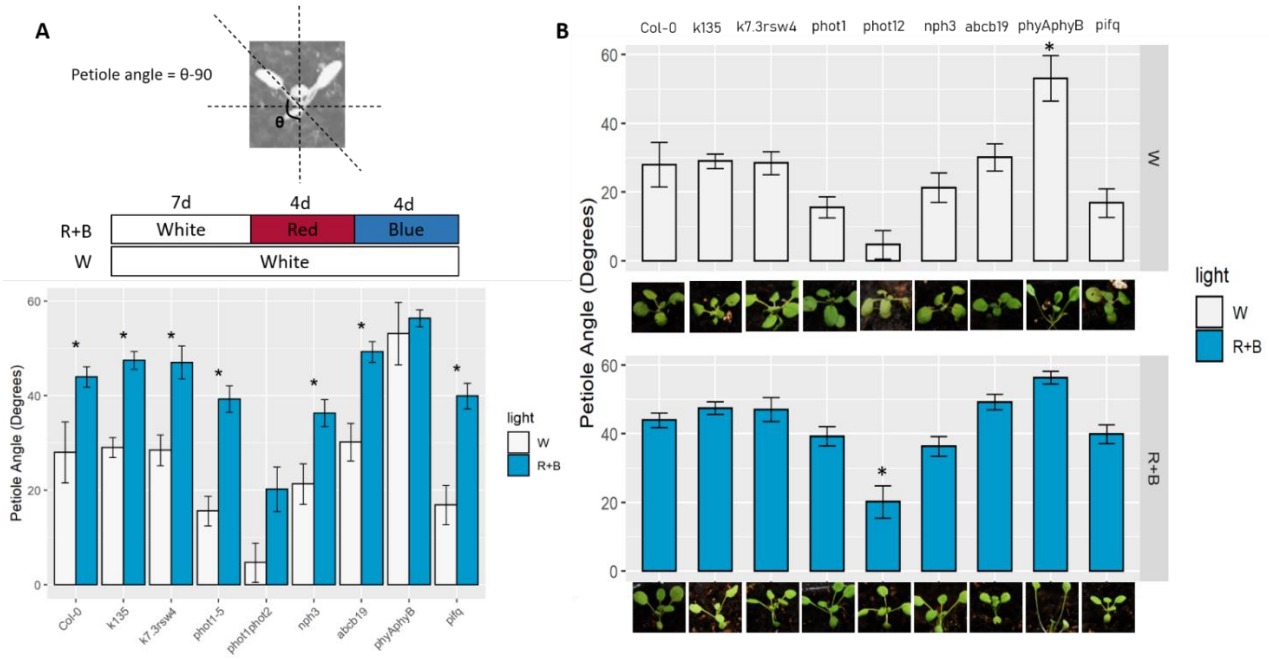

Figure 18. Involvement of KISC in regulating leaf positioning (b). Leaf positioning was determined after light treatments. Measurements done as described in Figure 17. Plants exposed to red light were transferred to blue light (R + B; 42 µmol m^{-2} s^{-1}; 16h photoperiod) or they remaining in white light (W; 150 µmol m^{-2} s^{-1}, 16h photoperiod) for additional 4 days. (A) grouping according to genotype (B) grouping according to light. Data shown represent means ± standard error (10 ≥ n ≥ 15). Asterisks indicate statistical difference by one-way ANOVA followed by Tukey's HSD (P < 0.05).

3.5 KISC is implicated in leaf flattening-curling response

PHOT1 (under low intensities of blue light) and phot2 (under high intensities of blue light) mediate leaf flattening, while nph3 has a central role in the signal transduction of phot1 (de Carbonnel et al., 2010; S. I. Inoue et al., 2008; Jenness et al., 2020). ABCB19 has recently been implicated in leaf morphology, however, no major defects in leaf flattening were reported in *abcb19* mutant after low or high blue light supplementation. This was because of the complex regulation of leaf flattening, that likely involves direct phot1 regulation of ABCB19 among several other auxin biosynthesis and transport processes (Jenness et al., 2020). Furthermore, the curled leaves in wild-type *Arabidopsis* grown under RL has been attributed to phyB Pfr, activated form, while it was shown that phototropins promote leaf flattening by suppressing the leaf-curling activity of phyB (Kozuka et al., 2013).

In order to access the involvement of KISC in leaf flattening, I grew plants under white light (150 µmol m^{-2} s^{-1}) in agar plates for 7 days, until reaching stage 1.02 (Boyes et al., 2001). Then, I transferred the seedling in soil and I kept them growing either under white (150 µmol m^{-2} s^{-1}, 16h photoperiod), red (105 µmol m^{-2} s^{-1}, 16h photoperiod) or blue (42 µmol m^{-2} s^{-1}, 16h photoperiod) LED light until they were 25 days old. Then I measured the leaf flattening index (see materials and methods) of the fifth rosette leaf of Col-0, *k135*, *k7.3rsw4*, *phot1-5*, *phot1-5 phot1-2*, *nph3*, *abcb19*, *phyA phyB* and *pifq* and I compared their flattening response in different light conditions, as well as the leaf flattening pattern among the different genotypes mentioned above (Figure 19).

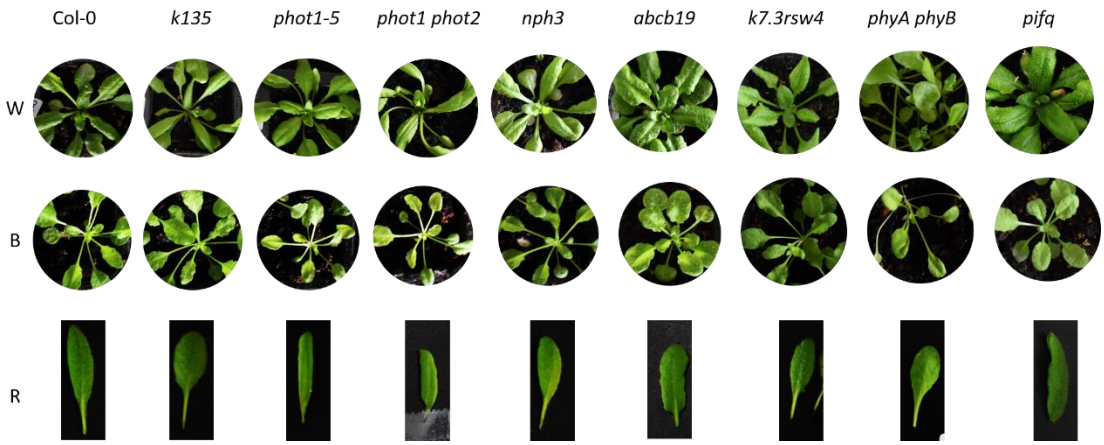

Figure 19. Rosette phenotypes of Col-0, *k135*, *k7.3rsw4*, *phot1-5*, *phot1-5 phot1-2*, *nph3*, *abcb19*, *phyA phyB* and *pifq*, growing under white (W; 150 µmol m^{-2} s^{-1}), blue (B; 42 µmol m^{-2} s^{-1}) or red (R; 105 µmol m^{-2} s^{-1}) LED light and 16h photoperiod. All the plants are 25days-old. In RL (third row) 5th rosette leaves are illustrated.

Interestingly, as shown in Figure 20A, under high intensity of white light, both *k135* and *k7.*3rsw4, together with *abcb19* exhibit more flattened leaves in the red than the white light condition. In contrast, all the other genotypes curling their leaves downwards in response to RL, with the exception of *phyA phyB* and *pifq* that, reasonably, are RL-insensitive.

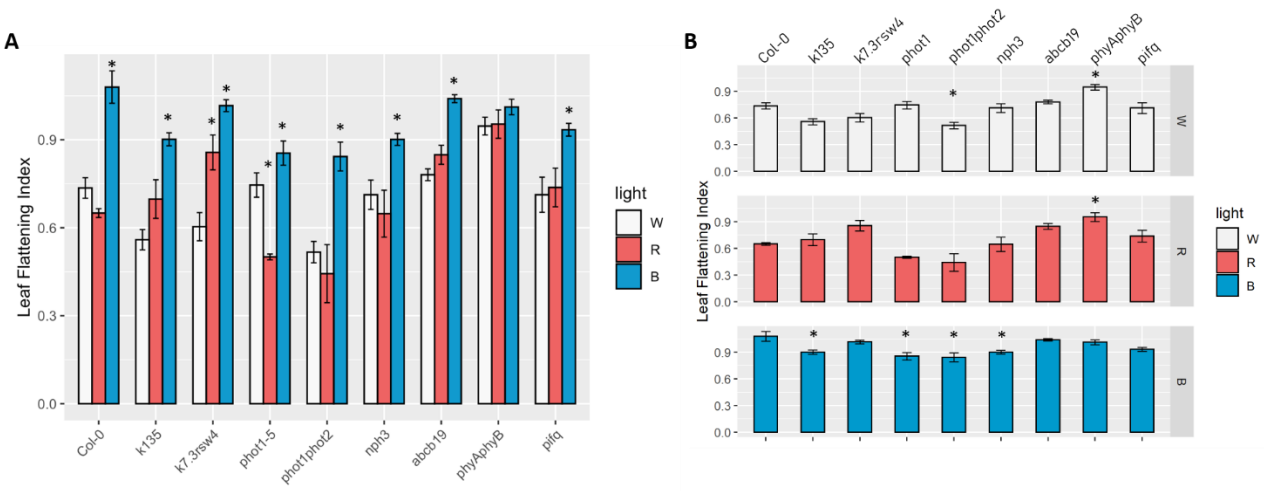

Figure 20. KISC seems to be involved in leaf flattening response. Plants were transferred from white light (7 days old) to either white, blue, or red LED-light, with 16h photoperiod, as described in materials and methods. When plants were 25 days old, the fifth rosette leaf of all the genotypes and replicates was measured for flattening index (curled leaf area deviated with manually flattened leaf area. Data shown are means ± SE ($5 \leq n \leq 12$). (A). Grouping by genotype. Asterisks indicate statistical difference detected by one-way ANOVA ($p < 0.05$) following by Tukey's HSD ($p < 0.05$), between different light conditions in the same genotype. (B). Grouping by light condition. Asterisks indicate statistical differences also detected by one-way ANOVA ($p < 0.05$) following by Tukey's HSD ($p < 0.05$), between genotypes versus Col-0.

Furthermore, looking at the differences between genotypes, *k135* and *k7.3rsw4* display more curling leaves with respect to WT, both under WL and RL. In contrast, BL alleviated differences between *phyA phyB* and *k135*, *k7.3rsw4*, *abcb19* and *pifq*, while *phot1-5*, *phot1-5 phot2-1*, and the phot1-related *nph3* showed statistically significant more curled phenotype comparing to Col-0 (Figure 20B). All together these data, demonstrate a possible crosstalk between phototropins and phyB in regulating leaf flattening, which has already been mentioned by Kozuka at al. (2013). Probably, phyB, either directly or indirectly, activates Kin7.3 downstream, to mediate leaf curling. On the other hand, phot1 may oppose this effect by physically interacting with Kin7.3. Thus, in RL, where phyB is active and phot1 is inactive, all the mutant lines, as well as Col-0, curl their leaves downwards, while *k135* and *k7.3rsw4* exhibit more flattened leaves. Additionally, the curled-leaf phenotype observed in white light conditions for *k7.3* mutant lines, points, in accordance with the literature, that phyB is genetically epistatic to PHOTs with respect to the curled-leaf phenotype. Finally, it is likely that the genetic crosstalk suggested for Kin7.3-phot1-phyB, also applies to ABCB19, as it displays the same pattern with Kin7.3 regarding the flattening-curling response. However, additional experiments should be done in order to validate all the above-mentioned hypothesis.

4 Discussion

The validation of the interaction between Kin7.3t and Phototropin1 (PHOT1), underlines the first evidence that KISC is involved in the light signaling transduction. As Kin7.3 is a core component of KISC and PHOT1 is the main photoreceptor responsible for BL and UV-A perception, the hypothesis that KISC plays a role in "blue-light pathways" is more than reasonable. Even though the interaction was not tested using the full-length Kin7.3, preliminary experiments through AP/MS (Kin7.3 interactome) conducted using full-length GFP-Kin7.3 suggest that Kin7.3 indeed can interact with PHOT1. Furthermore, ESP binds to the

C-terminal-tail domain of Kin7.3, relieving the self-inhibitory state of Kin7.3 in which the tail domain is "released" from the motor domain. Thus, the use of Kin7.3 which corresponds to the active open conformation of the tail domain is justified. It would be interesting, however, to test whether PHOT1-Kin7.3 interaction still occurs in *rsw4* (i.e. absence of ESP). Furthermore, regarding FHY3-Kin7.3 interaction, even though the Co-IP showed a "negative" result, the two proteins probably interact with each other transiently. Alternatively, the FHY3 could potentially interact with the Kin7.3 N-terminus, and thus the Co-IP conducted using Kin7.3 tail domain was inappropriate to detect the interaction. Thus, further evaluation needs to be done, either through cross-linking using appropriate constructs, or through enrichment of the active FHY3 form using RL after *N. benthamiana* agroinfiltration.

In order to investigate the *in vivo* PHOT1-Kin7.3 dynamics of colocalization, I proceeded with crossing PHOT1::PHOT1-GFP with Rps5a::tag-RFP-Kin7.3 (unpublished) transgenic plants. Seeds from T3 generation have already been collected and need to be checked under the confocal microscope in order to observe possible co-localization of tag-RFP-Kin7.3 and PHOT1-GFP. Other techniques for *in vivo* visualization of the interaction could also been conducted, such as Bimolecular fluorescence complementation (BiFC).

Regarding the physiological experiments conducted for the investigation of the pathways in which KISC is involved, it is important to clarify that all the above-mentioned results cannot validate that either *k135* or *k7.3 rsw4* phenotypic deviations from Col-0 (wild-type) are light-dependent. For instance, hyponasty response, which is strongly correlated with leaf positioning described by Inoue et al.(2008b), is not only manifested in shady conditions, but also upon different abiotic stresses such as flooding, mechanical stimulation and touching (thigmomorphogenesis), or elevated temperatures (Polko et al., 2011; Wit et al., 2012). Thus, it cannot be excluded that the increased petiole angles observed in *k7.3rsw4* were due to an abnormality caused in the expression of genes related to mechano-stimulation. In order to ensure the light-dependent phenotype, the crossed lines that have already been created (mutated background regarding both KISC-related and photoreceptor-related genes) should be subjected to the same experimental procedures. In this manner, the genetic relationship between KISC components and PHOT1, PHOT2, PHYB and PHYA photoreceptors could be evaluated either by rescued or enhanced phenotypes.

Nevertheless, in case that phenotypes observed upon leaf positioning and flattening experiments, are indeed light-dependent, we could propose a possible pathway which involves KISC, PHOT1, PHYB and indicates a potential crosstalk between the components. Regarding the leaf flattening response, as already mentioned, both *k135* and *k7.3rsw4* display a curling-leaf phenotype both in white and blue light conditions, unlike red light conditions in which rosette leaves were noticeably more flattened that the wild type. Taking into consideration, that in WL both PHYB and PHOT1 were active, and the knowledge that PHOT1 promotes leaf flattening by inhibiting PHYB leaf-curling activity (Kozuka et al., 2013), we can hypothesize that in *k135* and *k7.3rsw4*, PHOT1 signal transduction regarding this response was somehow inhibited. Furthermore, considering that in RL condition PHYB was in its Pfr active form and PHOT1 was inactive, we can also hypothesize that PHYB Pfr curling activity

was to some extend suppressed. Thus, we can assume that Kin7.3 and consequently KISC, is involved in the downstream signal initiated by PHYB in order for the leaves to be curled. In contrast, PHOT1 inhibits the signal transduction initiated by PHYB by physically interacting with Kin7.3. Finally, the still "curling" phenotype observed in both *k135* and *k7.3rsw4* in blue light conditions can be attributed by the assumption that phototropins not only mediate leaf flattening by preventing PHYB-dependent pathway, but may also act independently. The above-described crosstalk could potentially apply to the phenotype observed in *k7.3rsw4* mutants regarding leaf positioning. Probably, Kin7.3 acts downstream of PHYB Pfr in order for SAR to be suppressed.

Regarding the physiological experiments conducted using only BL of high intensity results should be reconsidered. I should point out that the experimental approach used for hypocotyl growth rate assay needs to be refined, as during imaging (10min intervals) exogenous WL light could get into the growth chamber. Thus, the data obtained for hypocotyl length and consequently hypocotyl growth rate in dark conditions contain artifacts, that could also explain the decreased hypocotyl length observed in all genotypes in darkness. Regarding phototropic experiments, even if the hyperbending response of *k135* and *k7.3 rsw4* is not attributed to PHOT1-Kin7.3 interaction, the KISC function in autotropism is of great importance, as it signals the termination of the phototropic response. Furthermore, it would be interesting to repeat the same experiment but without prior exposure to RL, in order to test if phytochromes are also responsible for the responses observed, as it has been shown that PHYA enhances hypocotyl curvature in etiolated seedlings (Haga et al., 2015). On the other hand, it would be very informative to assess the phototropic response in de-etiolated seedlings as described by Christie et al., (2011), where PHYB and PHOT1 display antagonistic action (Goyal et al., 2016), while seedlings are grown in light conditions that better resemble their natural environment.

Finally, with regards to the aforementioned phenotypes and physiological responses, we can assume that the involvement of KISC in light signaling is underlined by its role in regulating auxin canalization (Moschou et al., 2016). The establishment of an auxin gradient and the consequent asymmetric growth is of great importance for phototropism, leaf positioning and leaf flattening responses (J M Christie et al., 2011; Hansen et al., 2016; Hohm et al., 2013; Jenness et al., 2019, 2020; C. K. Pantazopoulou et al., 2017; Zhao et al., 2020). Indeed, in all physiological experiments and all light conditions tested, *k7.3rsw4* and *k135* display the same phenotypical pattern with ABCB19, which is an auxin efflux transporter. As ABCB19 and Kin7.3 directly interact with PHOT1, the hypothesis that PHOT1-ABCB19-Kin7.3 act in the same pathway to regulate light-dependent responses is strongly supported. ABCB19 control the auxin transport activity of PIN1 proteins by directly interacting with them and stabilize their localization in membrane microdomains at the plasma membrane in vivo and in yeast (Boosaree Titapiwatanakun et al., 2009). Moreover, ABCB19 tissue expression overlaps with that of PIN3 and PIN4 in the cortex, indicating that it could control the activities of many PIN transport pathways (revied in: Sakai & Haga, 2012). As KISC has been shown to control the polar localization of PINs in root system (Moschou et al., 2016), it would be possible to control the polar localization of PIN proteins in the aerial plant organs, too, such as leaves and stem.

Although the mechanism by which auxin induces differential cell growth either in stem (phototropism), petiole (hyponasty) or leaves (flattening) is not well understood (Bisgrove, 2008; Michaud et al., 2017; Zhao et al., 2020), it is thought that auxin alters the rate at which cells elongate by promoting cell wall extensibility (reviewed in: Bisgrove, 2008). In accordance, the RNAseq data analysis of *k135* showed that the GO term "plant-type cell wall organization or biogenesis" was highly enriched, while the respective genes (e.g. *EXPA16* and *EXPA2*, *XTH24*, XTH15) were up-regulated.

In conclusion, this study has contributed to the further clarification of the role of Kin7/Separase complex in aerial plant parts and the light signaling pathways. Additional experiments should be conducted in order to uncover the molecular mechanism under which KISC is implicated in the light-dependent signal transduction. Future studies could examine Kin7.3 expression pattern in leaves and stems of *Arabidopsis thaliana* in white, as well as in dark, red and blue light conditions of different intensities (at low and high photon fluence rates). Thus, it would be possible to better understand the expression pattern of Kin7.3 in different light conditions, and mainly, bypass the drawbacks of heterologous protein expression in *N. benthamiana*. Furthermore, using genetic tools available in the lab we could evaluate the genetic relationship between KISC components and different photoreceptors.

Finally, as already mentioned, the thorough comprehension of the mechanisms underlying light signaling, could lead to multiple applications in agriculture, either through the exploitation of transgenic plants exhibit a gain of function phenotype regarding light capture and thus photosynthesis, or by using light-controlled environments, in which crops could grow in more favorable conditions. For instance, *kin7.3 rsw4* does not seem to exhibit a typical shade avoidance response (SAR), which could be of great importance for agriculture. Numerus studies indicate that SAR leads to an increased photosynthetic capacity essential for light competition among plants (Weiner et al., 2001; Pantazopoulou et al., 2019). On the other hand, the apical dominance observed as adaptation in shady environments, induces reallocation of resources into elongation growth at the expense of harvestable organs (usually fruits and seeds) (Roig-Villanova & Martínez-García, 2016). This investment inevitably leads to a decrease in crop yield (Boccalandro et al., 2003). *kin7.3rsw4* mutant line displays a constitutive hyponasty response, as already shown, but also delayed flowering (data not shown). On the other hand, transgenic plants could be beneficial for agro-economy not only at the level of transgenic crops (directly), but also at the level of cultivations. Using appropriate combination of crops and gain-of-function-transgenic plants regarding light capture, favorable crop patterns could be applied in order, for example to suppress weeds' development by subjecting them in continuous shady environments, detrimental for their development.

5 References

Ballaré, C. L., & Pierik, R. (2017). The shade-avoidance syndrome: Multiple signals and ecological consequences. *Plant Cell and Environment*, *40*(11), 2530–2543. https://doi.org/10.1111/pce.12914

Bisgrove, S. R. (2008). The roles of microtubules in tropisms. *Plant Science*, *175*(6), 747–755. https://doi.org/10.1016/j.plantsci.2008.08.009

Boccalandro, H. E., Ploschuk, E. L., Yanovsky, M. J., Sánchez, R. A., Gatz, C., & Casal, J. J. (2003). Increased Phytochrome B Alleviates Density Effects on Tuber Yield of Field Potato Crops. *Plant Physiology*, *133*(4), 1539–1546. https://doi.org/10.1104/pp.103.029579

Bontinck, M., Van Leene, J., Gadeyne, A., De Rybel, B., Eeckhout, D., Nelissen, H., & De Jaeger, G. (2018). Recent trends in plant protein complex analysis in a developmental context. *Frontiers in Plant Science*, *9*(May), 1–14. https://doi.org/10.3389/fpls.2018.00640

Boyes, D. C., Zayed, A. M., Ascenzi, R., McCaskill, A. J., Hoffman, N. E., Davis, K. R., & Görlach, J. (2001). Growth stage-based phenotypic analysis of Arabidopsis: A model for high throughput functional genomics in plants. *Plant Cell*, *13*(7), 1499–1510. https://doi.org/10.1105/tpc.13.7.1499

Briggs, W. R., & Christie, J. M. (2002). Phototropins 1 and 2: Versatile plant blue-light receptors. *Trends in Plant Science*, *7*(5), 204–210. https://doi.org/10.1016/S1360-1385(02)02245-8

Casal, J. J. (2012). Shade Avoidance. *The Arabidopsis Book*, *10*, e0157. https://doi.org/10.1199/tab.0157

Casal, J. J. (2013). Photoreceptor Signaling Networks in Plant Responses to Shade. *Annual Review of Plant Biology*, *64*(1), 403–427. https://doi.org/10.1146/annurev-arplant-050312-120221

Christie, J M, Yang, H., Richter, G. L., Sullivan, S., Thomson, C. E., Lin, J., Titapiwatanakun, B., Ennis, M., Kaiserli, E., Lee, O. R., Adamec, J., Peer, W. A., & Murphy, A. S. (2011). phot1 inhibition of ABCB19 primes lateral auxin fluxes in the shoot apex required for phototropism. *PLoS Biol*, *9*(6), e1001076. https://doi.org/10.1371/journal.pbio.1001076

Christie, John M. (2007). Phototropin Blue-Light Receptors. *Annual Review of Plant Biology*, *58*(1), 21–45. https://doi.org/10.1146/annurev.arplant.58.032806.103951

Christie, John M., Blackwood, L., Petersen, J., & Sullivan, S. (2015). Plant flavoprotein photoreceptors. *Plant and Cell Physiology*, *56*(3), 401–413. https://doi.org/10.1093/pcp/pcu196

Christie, John M., & Murphy, A. S. (2013). Shoot phototropism in higher plants: New light through old concepts. *American Journal of Botany*, *100*(1), 35–46. https://doi.org/10.3732/ajb.1200340

Christie, John M., Reymond, P., Powell, G. K., Bernasconi, P., Raibekas, A. A., Liscum, E., & Briggs, W. R. (1998). Arabidopsis NPH1: A flavoprotein with the properties of a photoreceptor for phototropism. *Science*, *282*(5394), 1698–1701. https://doi.org/10.1126/science.282.5394.1698

Christie, John M., Suetsugu, N., Sullivan, S., & Wada, M. (2018). Shining light on the function of nph3/rpt2-like proteins in phototropin signaling. *Plant Physiology*, *176*(2), 1015–1024. https://doi.org/10.1104/pp.17.00835

de Campos, M. K. F., & Schaaf, G. (2017). The regulation of cell polarity by lipid transfer proteins of the SEC14 family. *Curr Opin Plant Biol*, *40*, 158–168. https://doi.org/10.1016/j.pbi.2017.09.007

de Carbonnel, M., Davis, P., Roelfsema, M. R. G., Inoue, S. I., Schepens, I., Lariguet, P., Geisler, M., Shimazaki, K. I., Hangarter, R., & Fankhauser, C. (2010). The Arabidopsis PHYTOCHROME KINASE SUBSTRATE2 protein is a phototropin signaling element that regulates leaf flattening and leaf positioning. *Plant Physiology*, *152*(3), 1391–1405. https://doi.org/10.1104/pp.109.150441

de Wit, M., Keuskamp, D. H., Bongers, F. J., Hornitschek, P., Gommers, C. M. M., Reinen, E., Martínez-Cerón, C., Fankhauser, C., & Pierik, R. (2016). Integration of Phytochrome and Cryptochrome Signals Determines Plant Growth during Competition for Light. *Current Biology*, *26*(24), 3320–3326. https://doi.org/10.1016/j.cub.2016.10.031

Demarsy, E., Schepens, I., Okajima, K., Hersch, M., Bergmann, S., Christie, J., Shimazaki, K. I., Tokutomi, S., & Fankhauser, C. (2012). Phytochrome Kinase Substrate 4 is phosphorylated by the phototropin 1 photoreceptor. *EMBO Journal*, *31*(16), 3457–3467. https://doi.org/10.1038/emboj.2012.186

Ding, Z., Galvan-Ampudia, C. S., Demarsy, E., Langowski, L., Kleine-Vehn, J., Fan, Y., Morita, M. T., Tasaka, M., Fankhauser, C., Offringa, R., & Friml, J. (2011). Light-mediated polarization of the PIN3

auxin transporter for the phototropic response in Arabidopsis. *Nature Cell Biology*, *13*(4), 447–452. https://doi.org/10.1038/ncb2208

Fankhauser, C., & Christie, J. M. (2015). Plant phototropic growth. *Current Biology*, *25*(9), R384–R389. https://doi.org/10.1016/j.cub.2015.03.020

Folta, K. M., & Spalding, E. P. (2001). Unexpected roles for cryptochrome 2 and phototropin revealed by high-resolution analysis of blue light-mediated hypocotyl growth inhibition. *Plant Journal*, *26*(5), 471–478. https://doi.org/10.1046/j.1365-313X.2001.01038.x

Folta, Kevin M., & Kaufman, L. S. (2003). Phototropin 1 is required for high-fluence blue-light-mediated mRNA destabilization. *Plant Molecular Biology*, *51*(4), 609–618. https://doi.org/10.1023/A:1022393406204

Folta, Kevin M., Lieg, E. J., Durham, T., & Spalding, E. P. (2003). Primary Inhibition of Hypocotyl Growth and Phototropism Depend Differently on Phototropin-Mediated Increases in Cytoplasmic Calcium Induced by Blue Light. *Plant Physiology*, *133*(4), 1464–1470. https://doi.org/10.1104/pp.103.024372

Fraser, D. P., Hayes, S., & Franklin, K. A. (2016). Photoreceptor crosstalk in shade avoidance. *Current Opinion in Plant Biology*, *33*, 1–7. https://doi.org/10.1016/j.pbi.2016.03.008

Ghosh, R., de Campos, M. K., Huang, J., Huh, S. K., Orlowski, A., Yang, Y., Tripathi, A., Nile, A., Lee, H. C., Dynowski, M., Schafer, H., Rog, T., Lete, M. G., Ahyayauch, H., Alonso, A., Vattulainen, I., Igumenova, T. I., Schaaf, G., & Bankaitis, V. A. (2015). Sec14-nodulin proteins and the patterning of phosphoinositide landmarks for developmental control of membrane morphogenesis. *Mol Biol Cell*, *26*(9), 1764–1781. https://doi.org/10.1091/mbc.E14-10-1475

Goyal, A., Karayekov, E., Galvão, V. C., Ren, H., Casal, J. J., & Fankhauser, C. (2016a). Shade Promotes Phototropism through Phytochrome B-Controlled Auxin Production. *Current Biology*, *26*(24), 3280–3287. https://doi.org/10.1016/j.cub.2016.10.001

Goyal, A., Karayekov, E., Galvão, V. C., Ren, H., Casal, J. J., & Fankhauser, C. (2016b). Shade Promotes Phototropism through Phytochrome B-Controlled Auxin Production. *Current Biology*, *26*(24), 3280–3287. https://doi.org/10.1016/j.cub.2016.10.001

Goyal, A., Szarzynska, B., & Fankhauser, C. (2013). Phototropism: At the crossroads of light-signaling pathways. *Trends in Plant Science*, *18*(7), 393–401. https://doi.org/10.1016/j.tplants.2013.03.002

Guan, C., Wu, B., Yu, T., Wang, Q., Krogan, N. T., Liu, X., & Jiao, Y. (2017). Spatial Auxin Signaling Controls Leaf Flattening in Arabidopsis. *Current Biology*, *27*(19), 2940-2950.e4. https://doi.org/10.1016/j.cub.2017.08.042

Haga, K., Tsuchida-Mayama, T., Yamada, M., & Sakai, T. (2015). Arabidopsis ROOT PHOTOTROPISM2 contributes to the adaptation to high-intensity light in phototropic responses. *Plant Cell*, *27*(4), 1098–1112. https://doi.org/10.1105/tpc.15.00178

Hansen, J. S., Krintel, C., Hernebring, M., Haataja, T. J., de Mare, S., Wasserstrom, S., Kosinska-Eriksson, U., Palmgren, M., Holm, C., Stenkula, K. G., Jones, H. A., & Lindkvist-Petersson, K. (2016). Perilipin 1 binds to aquaporin 7 in human adipocytes and controls its mobility via protein kinase A mediated phosphorylation. *Metabolism*, *65*(12), 1731–1742. https://doi.org/10.1016/j.metabol.2016.09.004

Harada, A., & Shimazaki, K. (2007). Phototropins and Blue Light-dependent Calcium Signaling in Higher Plants†. *Photochemistry and Photobiology*, *83*(1), 102–111. https://doi.org/10.1562/2006-03-08-ir-837

Harada, A., Takemiya, A., Inoue, S. I., Sakai, T., & Shimazaki, K. I. (2013). Role of RPT2 in leaf positioning and flattening and a possible inhibition of phot2 signaling by phot1. *Plant and Cell Physiology*, *54*(1), 36–47. https://doi.org/10.1093/pcp/pcs094

Hayes, S., Velanis, C. N., Jenkins, G. I., & Franklin, K. A. (2014). UV-B detected by the UVR8

photoreceptor antagonizes auxin signaling and plant shade avoidance. *Proceedings of the National Academy of Sciences of the United States of America*, *111*(32), 11894–11899. https://doi.org/10.1073/pnas.1403052111

Heijde, M., & Ulm, R. (2012). UV-B photoreceptor-mediated signalling in plants. *Trends in Plant Science*, *17*(4), 230–237. https://doi.org/10.1016/j.tplants.2012.01.007

Hohm, T., Preuten, T., & Fankhauser, C. (2013). Phototropism: Translating light into directional growth. *American Journal of Botany*, *100*(1), 47–59. https://doi.org/10.3732/ajb.1200299

Huber, M., Nieuwendijk, N. M., Pantazopoulou, C. K., & Pierik, R. (2020). Light signalling shapes plant–plant interactions in dense canopies. *Plant Cell and Environment*, *October*, 1–16. https://doi.org/10.1111/pce.13912

Inoue, S. I., Kinoshita, T., Takemiya, A., Doi, M., & Shimazaki, K. I. (2008). Leaf positioning of Arabidopsis in response to blue light. *Molecular Plant*, *1*(1), 15–26. https://doi.org/10.1093/mp/ssm001

Inoue, S. ichiro, Takemiya, A., & Shimazaki, K. ichiro. (2010). Phototropin signaling and stomatal opening as a model case. *Current Opinion in Plant Biology*, *13*(5), 587–593. https://doi.org/10.1016/j.pbi.2010.09.002

Jenkins, G. I. (2017). Photomorphogenic responses to ultraviolet-B light. *Plant Cell and Environment*. https://doi.org/10.1111/pce.12934

Jenness, M. K., Carraro, N., Pritchard, C. A., & Murphy, A. S. (2019). The arabidopsis ATP-BINDING CASSETTE transporter ABCB21 regulates auxin levels in cotyledons, the root pericycle, and leaves. *Frontiers in Plant Science*, *10*(June), 1–14. https://doi.org/10.3389/fpls.2019.00806

Jenness, M. K., Tayengwa, R., & Murphy, A. S. (2020). An ATP-binding cassette transporter, ABCB19, regulates leaf position and morphology during phototropin1-mediated blue light responses. *Plant Physiology*, *184*(November), pp.00223.2020. https://doi.org/10.1104/pp.20.00223

Kagawa, T., Sakai, T., Suetsugu, N., Oikawa, K., Ishiguro, S., Kato, T., Tabata, S., Okada, K., & Wada, M. (2001). Arabidopsis NPL1: A phototropin homolog controlling the chloroplast high-light avoidance response. *Science*, *291*(5511), 2138–2141. https://doi.org/10.1126/science.291.5511.2138

Kami, C., Lorrain, S., Hornitschek, P., & Fankhauser, C. (2010). Light-regulated plant growth and development. *Current Topics in Developmental Biology*, *91*(C), 29–66. https://doi.org/10.1016/S0070-2153(10)91002-8

Kimura, T., Tsuchida-mayama, T., Imai, H., Okajima, K., Ito, K., & Business, K. (2020). Arabidopsis ROOT PHOTOTROPISM2 Is a Light-Dependent Dynamic Modulator of Phototropin1. *Plant Cell*. https://doi.org/10.1105/tpc.19.00926

Kinoshita, T., Doi, M., & Suetsugu, N. (2001). Regulation of Stomatal Opening. *Nature*, *414*(December), 0–4.

Kong, Y., & Zheng, Y. (2020). Phototropin is partly involved in blue-light-mediated stem elongation, flower initiation, and leaf expansion: A comparison of phenotypic responses between wild Arabidopsis and its phototropin mutants. *Environmental and Experimental Botany*, *171*(December 2019), 103967. https://doi.org/10.1016/j.envexpbot.2019.103967

Kozuka, T., Suetsugu, N., Wada, M., & Nagatani, A. (2013). Antagonistic regulation of leaf flattening by phytochrome B and phototropin in Arabidopsis thaliana. *Plant and Cell Physiology*, *54*(1), 69–79. https://doi.org/10.1093/pcp/pcs134

Legris, M., & Boccaccini, A. (2020). Stem phototropism toward blue and ultraviolet light. *Physiologia Plantarum*, *169*(3), 357–368. https://doi.org/10.1111/ppl.13098

Legris, M., Ince, Y. Ç., & Fankhauser, C. (2019). Molecular mechanisms underlying phytochrome-controlled morphogenesis in plants. *Nature Communications*, *10*(1). https://doi.org/10.1038/s41467-019-13045-0

Leivar, P., Tepperman, J. M., Cohn, M. M., Monte, E., Al-Sady, B., Erickson, E., & Quail, P. H. (2012). Dynamic antagonism between phytochromes and PIF family basic helix-loop-helix factors induces selective reciprocal responses to light and shade in a rapidly responsive transcriptional network in Arabidopsis. *Plant Cell*, *24*(4), 1398–1419. https://doi.org/10.1105/tpc.112.095711

Li, F. W., Rothfels, C. J., Melkonian, M., Villarreal, J. C., Stevenson, D. W., Graham, S. W., Wong, G. K. S., Mathews, S., & Pryer, K. M. (2015). The origin and evolution of phototropins. *Frontiers in Plant Science*, *6*(AUG), 1–11. https://doi.org/10.3389/fpls.2015.00637

Li, L., Ljung, K., Breton, G., Schmitz, R. J., Pruneda-Paz, J., Cowing-Zitron, C., Cole, B. J., Ivans, L. J., Pedmale, U. V, Jung, H. S., Ecker, J. R., Kay, S. A., & Chory, J. (2012). Linking photoreceptor excitation to changes in plant architecture. *Genes & Development*, *26*(8), 785–790. https://doi.org/10.1101/gad.187849.112

Lian, H. L., He, S. B., Zhang, Y. C., Zhu, D. M., Zhang, J. Y., Jia, K. P., Sun, S. X., Li, L., & Yang, H. Q. (2011). Blue-light-dependent interaction of cryptochrome 1 with SPA1 defines a dynamic signaling mechanism. *Genes and Development*, *25*(10), 1023–1028. https://doi.org/10.1101/gad.2025111

Lindeboom, J. J., Nakamura, M., Hibbel, A., Gutierrez, R., Ketelaar, T., Emons, A. M. C., Bela, M., Kirik, V., & Ehrhardt, D. W. (2013). A Mechanism for Reorientation of Cortical Microtubule Arrays Driven by Microtubule Severing. *Science*, *342*(6163), 1245533. http://eutils.ncbi.nlm.nih.gov/entrez/eutils/elink.fcgi?dbfrom=pubmed&id=24200811&retmode=ref&cmd=prlinks%0Afile:///Files/5D/5DD1F345-4041-487D-973E-9B40313E3B42.pdf%0Apapers3://publication/doi/10.1126/science.1245533

Liscum, E. (2016). Blue light-induced intracellular movement of phototropins: Functional relevance or red herring? *Frontiers in Plant Science*, *7*(June2016), 1–5. https://doi.org/10.3389/fpls.2016.00827

Liscum, E., Askinosie, S. K., Leuchtman, D. L., Morrow, J., Willenburg, K. T., & Coats, D. R. (2014). Phototropism: Growing towards an understanding of plant movement. *Plant Cell*, *26*(1), 38–55. https://doi.org/10.1105/tpc.113.119727

Liu, Y., Wei, H., Ma, M., Li, Q., Kong, D., Sun, J., Ma, X., Wang, B., Chen, C., Xie, Y., & Wang, H. (2019). Arabidopsis FHY3 and FAR1 regulate the balance between growth and defense responses under shade conditions. *Plant Cell*, *31*(9), 2089–2106. https://doi.org/10.1105/TPC.18.00991

Liu, Z., & Makaroff, C. A. (2006). Arabidopsis separase AESP is essential for embryo development and the release of cohesin during meiosis. *Plant Cell*, *18*(5), 1213–1225. https://doi.org/10.1105/tpc.105.036913

Michaud, O., Fiorucci, A.-S., Xenarios, I., & Fankhauser, C. (2017). *Local auxin production underlies a spatially restricted neighbor-detection response in Arabidopsis*. *114*(28), 7444–7449. https://doi.org/10.1073/pnas.1702276114 %J Proceedings of the National Academy of Sciences

Millenaar, F. F., Van Zanten, M., Cox, M. C. H., Pierik, R., Voesenek, L. A. C. J., & Peeters, A. J. M. (2009). Differential petiole growth in Arabidopsis thaliana: Photocontrol and hormonal regulation. *New Phytologist*, *184*(1), 141–152. https://doi.org/10.1111/j.1469-8137.2009.02921.x

Moschou, P N, & Bozhkov, P. V. (2012). Separases: biochemistry and function. *Physiol Plant*, *145*(1), 67–76. https://doi.org/10.1111/j.1399-3054.2011.01550.x

Moschou, P N, Gutierrez-Beltran, E., Bozhkov, P. V, & Smertenko, A. (2016). Separase Promotes Microtubule Polymerization by Activating CENP-E-Related Kinesin Kin7. *Dev Cell*, *37*(4), 350–361. https://doi.org/10.1016/j.devcel.2016.04.015

Moschou, P N, Smertenko, A. P., Minina, E. A., Fukada, K., Savenkov, E. I., Robert, S., Hussey, P. J., & Bozhkov, P. V. (2013). The caspase-related protease separase (extra spindle poles) regulates cell polarity and cytokinesis in Arabidopsis. *Plant Cell*, *25*(6), 2171–2186. https://doi.org/10.1105/tpc.113.113043

Moschou, Panagiotis N., Gutierrez-Beltran, E., Bozhkov, P. V., & Smertenko, A. (2016). Separase Promotes Microtubule Polymerization by Activating CENP-E-Related Kinesin Kin7. *Developmental Cell*, *37*(4), 350–361. https://doi.org/10.1016/j.devcel.2016.04.015

Motchoulski, A., & Liscum, E. (1999). Arabidopsis NPH3: A NPH1 photoreceptor-interacting protein essential for phototropism. *Science*, *286*(5441), 961–964. https://doi.org/10.1126/science.286.5441.961

Mullen, J. L., Weinig, C., & Hangarter, R. P. (2006). Shade avoidance and the regulation of leaf inclination in Arabidopsis. *Plant Cell and Environment*, *29*(6), 1099–1106. https://onlinelibrary.wiley.com/doi/pdf/10.1111/j.1365-3040.2005.01484.x

Okamoto, K., Ueda, H., Shimada, T., Tamura, K., Kato, T., Tasaka, M., Morita, M. T., & Hara-Nishimura, I. (2015). Regulation of organ straightening and plant posture by an actin–myosin XI cytoskeleton. *Nature Plants*, *1*(4), 15031. https://doi.org/10.1038/nplants.2015.31

Pantazopoulou, C. (2017). *Mechanisms and consequences of neighbour detection in Arabidopsis thaliana*. www.ridderprint.nl

Pantazopoulou, C. K., Bongers, F. J., Küpers, J. J., Reinen, E., Das, D., Evers, J. B., Anten, N. P. R., & Pierik, R. (2017). Neighbor detection at the leaf tip adaptively regulates upward leaf movement through spatial auxin dynamics. *Proceedings of the National Academy of Sciences of the United States of America*, *114*(28), 7450–7455. https://doi.org/10.1073/pnas.1702275114

Pantazopoulou, C. K., Bongers, F. J., & Pierik, R. (2019). Plant Ecophysiology, Dept. of Biology, Utrecht University, The Netherlands State Key Laboratory of Vegetation and Environmental Change, Institute of Botany, Chinese Academy of Sciences, Beijing, China. *BioRx*, 1–23.

Parks, B. M., Quail, P. H., & Hangarter, R. P. (1996). Phytochrome A regulates red-light induction of phototropic enhancement in Arabidopsis. *Plant Physiology*, *110*(1), 155–162. https://doi.org/10.1104/pp.110.1.155

Pedmale, U. V., Huang, S. S. C., Zander, M., Cole, B. J., Hetzel, J., Ljung, K., Reis, P. A. B., Sridevi, P., Nito, K., Nery, J. R., Ecker, J. R., & Chory, J. (2016). Cryptochromes Interact Directly with PIFs to Control Plant Growth in Limiting Blue Light. *Cell*, *164*(1–2), 233–245. https://doi.org/10.1016/j.cell.2015.12.018

Pedmale, U. V., & Liscum, E. (2007a). Regulation of phototropic signaling in Arabidopsis via phosphorylation state changes in the phototropin 1-interacting protein NPH3. *Journal of Biological Chemistry*, *282*(27), 19992–20001. https://doi.org/10.1074/jbc.M702551200

Pedmale, U. V., & Liscum, E. (2007b). Regulation of phototropic signaling in Arabidopsis via phosphorylation state changes in the phototropin 1-interacting protein NPH3. *Journal of Biological Chemistry*, *282*(27), 19992–20001. https://doi.org/10.1074/jbc.M702551200

Pfeifer, A., Mathes, T., Lu, Y., Hegemann, P., & Kottke, T. (2010). Blue light induces global and localized conformational changes in the kinase domain of full-length phototropin. *Biochemistry*, *49*(5), 1024–1032. https://doi.org/10.1021/bi9016044

Pierik, R., & De Wit, M. (2014). Shade avoidance: Phytochrome signalling and other aboveground neighbour detection cues. *Journal of Experimental Botany*, *65*(11), 2815–2824. https://doi.org/10.1093/jxb/ert389

Polko, J. K., Voesenek, L. A. C. J., Peeters, A. J. M., & Pierik, R. (2011). Petiole hyponasty: An ethylene-driven, adaptive response to changes in the environment. *AoB PLANTS*, *11*(1), 1–11. https://doi.org/10.1093/aobpla/plr031

Preuten, T., Blackwood, L., Christie, J. M., & Fankhauser, C. (2015). Lipid anchoring of arabidopsis phototropin 1 to assess the functional significance of receptor internalization: Should I stay or should I go? *New Phytologist*, *206*(3), 1038–1050. https://doi.org/10.1111/nph.13299

Queralt, E., Lehane, C., Novak, B., & Uhlmann, F. (2006). Downregulation of PP2A(Cdc55) phosphatase

by separase initiates mitotic exit in budding yeast. *Cell*, *125*(4), 719–732. https://doi.org/10.1016/j.cell.2006.03.038

Reichel, M., Liao, Y., Rettel, M., Ragan, C., Evers, M., Alleaume, A. M., Horos, R., Hentze, M. W., Preiss, T., & Millar, A. A. (2016). In planta determination of the mRNA-binding proteome of arabidopsis etiolated seedlings. *Plant Cell*, *28*(10), 2435–2452. https://doi.org/10.1105/tpc.16.00562

Rizzini, L., Favory, J. J., Cloix, C., Faggionato, D., O'Hara, A., Kaiserli, E., Baumeister, R., Schäfer, E., Nagy, F., Jenkins, G. I., & Ulm, R. (2011). Perception of UV-B by the arabidopsis UVR8 protein. *Science*, *332*(6025), 103–106. https://doi.org/10.1126/science.1200660

Roberts, D., Pedmale, U. V., Morrow, J., Sachdev, S., Lechner, E., Tang, X., Zheng, N., Hannink, M., Genschik, P., & Liscum, E. (2011). Modulation of phototropic responsiveness in arabidopsis through ubiquitination of phototropin 1 by the CUL3-ring E3 ubiquitin ligase CRL3 NPH3. *Plant Cell*, *23*(10), 3627–3640. https://doi.org/10.1105/tpc.111.087999

Roig-Villanova, I., & Martínez-García, J. F. (2016). Plant responses to vegetation proximity: A whole life avoiding shade. *Frontiers in Plant Science*, *7*(FEB2016), 1–10. https://doi.org/10.3389/fpls.2016.00236

Rubio, V., Shen, Y., Saijo, Y., Liu, Y., Gusmaroli, G., Dinesh-Kumar, S. P., & Deng, X. W. (2005). An alternative tandem affinity purification strategy applied to Arabidopsis protein complex isolation. *Plant Journal*, *41*(5), 767–778. https://doi.org/10.1111/j.1365-313X.2004.02328.x

Sakai, T., & Haga, K. (2012). Molecular genetic analysis of phototropism in arabidopsis. *Plant and Cell Physiology*, *53*(9), 1517–1534. https://doi.org/10.1093/pcp/pcs111

Sakai, T., Kagawa, T., Kasahara, M., Swartz, T. E., Christie, J. M., Briggs, W. R., Wada, M., & Okada, K. (2001). Arabidopsis nph1 and npl1: Blue light receptors that mediate both phototropism and chloroplast relocation. *Proceedings of the National Academy of Sciences of the United States of America*, *98*(12), 6969–6974. https://doi.org/10.1073/pnas.101137598

Sakamoto, K., & Briggs, W. R. (2002). Cellular and subcellular localization of phototropin 1. *Plant Cell*, *14*(8), 1723–1735. https://doi.org/10.1105/tpc.003293

Schumacher, P., Demarsy, E., Waridel, P., Petrolati, L. A., Trevisan, M., & Fankhauser, C. (2018). A phosphorylation switch turns a positive regulator of phototropism into an inhibitor of the process. *Nature Communications*, *9*(1), 1–9. https://doi.org/10.1038/s41467-018-04752-1

Sharma, A., Sharma, B., Hayes, S., Kerner, K., Hoecker, U., Jenkins, G. I., & Franklin, K. A. (2019). UVR8 disrupts stabilisation of PIF5 by COP1 to inhibit plant stem elongation in sunlight. *Nature Communications*, *10*(1), 4417. https://doi.org/10.1038/s41467-019-12369-1

Sheerin, D. J., Menon, C., Oven-Krockhaus, S. Zur, Enderle, B., Zhu, L., Johnen, P., Schleifenbaum, F., Stierhof, Y. D., Huq, E., & Hiltbrunner, A. (2015). Light-activated phytochrome A and B interact with members of the SPA family to promote photomorphogenesis in arabidopsis by reorganizing the COP1/SPA complex. *Plant Cell*, *27*(1), 189–201. https://doi.org/10.1105/tpc.114.134775

Siddiqui, H., Khan, S., Rhodes, B. M., & Devlin, P. F. (2016). FHY3 and FAR1 act downstream of light stable phytochromes. *Frontiers in Plant Science*, *7*(FEB2016), 1–10. https://doi.org/10.3389/fpls.2016.00175

Smith, H., & Whitelam, G. C. (1997). The shade avoidance syndrome: Multiple responses mediated by multiple phytochromes. *Plant, Cell and Environment*, *20*(6), 840–844. https://doi.org/10.1046/j.1365-3040.1997.d01-104.x

Smith, Harry. (1982). *STRATEGY*. 481–518.

Sullivan, S., Kaiserli, E., Tseng, T. S., & Christie, J. M. (2010). Subcellular localization and turnover of Arabidopsis phototropin 1. *Plant Signaling and Behavior*, *5*(2), 184–186. https://doi.org/10.4161/psb.5.2.11082

Sullivan, S., Kharshiing, E., Laird, J., Sakai, T., & Christie, J. M. (2019a). Deetiolation enhances phototropism by modulating non-phototropic hypocotyl3.Phosphorylation status. *Plant Physiology*, *180*(2), 1119–1131. https://doi.org/10.1104/pp.19.00206

Sullivan, S., Kharshiing, E., Laird, J., Sakai, T., & Christie, J. M. (2019b). Deetiolation enhances phototropism by modulating non-phototropic hypocotyl3.Phosphorylation status. *Plant Physiology*, *180*(2), 1119–1131. https://doi.org/10.1104/pp.19.00206

Takemiya, A., Inoue, S. I., Doi, M., Kinoshita, T., & Shimazaki, K. I. (2005). Phototropins promote plant growth in response to blue light in low light environments. *Plant Cell*, *17*(4), 1120–1127. https://doi.org/10.1105/tpc.104.030049

Titapiwatanakun, B, & Murphy, A. S. (2009). Post-transcriptional regulation of auxin transport proteins: cellular trafficking, protein phosphorylation, protein maturation, ubiquitination, and membrane composition. *J Exp Bot*, *60*(4), 1093–1107. https://doi.org/10.1093/jxb/ern240

Titapiwatanakun, Boosaree, Blakeslee, J. J., Bandyopadhyay, A., Yang, H., Mravec, J., Sauer, M., Cheng, Y., Adamec, J., Nagashima, A., Geisler, M., Sakai, T., Friml, J., Peer, W. A., & Murphy, A. S. (2009). ABCB19/PGP19 stabilises PIN1 in membrane microdomains in Arabidopsis. *Plant Journal*, *57*(1), 27–44. https://doi.org/10.1111/j.1365-313X.2008.03668.x

Titeca, K., Lemmens, I., Tavernier, J., & Eyckerman, S. (2019). Discovering cellular protein-protein interactions: Technological strategies and opportunities. *Mass Spectrometry Reviews*, *38*(1), 79–111. https://doi.org/10.1002/mas.21574

Toledo-Ortiz, G., Johansson, H., Lee, K. P., Bou-Torrent, J., Stewart, K., Steel, G., Rodríguez-Concepción, M., & Halliday, K. J. (2014). The HY5-PIF Regulatory Module Coordinates Light and Temperature Control of Photosynthetic Gene Transcription. *PLoS Genetics*, *10*(6). https://doi.org/10.1371/journal.pgen.1004416

Wan, Y. L., Eisinger, W., Ehrhardt, D., Kubitscheck, U., Baluska, F., & Briggs, W. (2008). The subcellular localization and blue-light-induced movement of phototropin 1-GFP in etiolated seedlings of Arabidopsis thaliana. *Molecular Plant*, *1*(1), 103–117. https://doi.org/10.1093/mp/ssm011

Wang, X., Gao, X., Liu, Y., Fan, S., & Ma, Q. (2020). Progress of Research on the Regulatory Pathway of the Plant Shade-Avoidance Syndrome. *Frontiers in Plant Science*, *11*(April), 1–12. https://doi.org/10.3389/fpls.2020.00439

Weiner, J., Griepentrog, H. W., & Kristensen, L. (2001). Suppression of weeds by spring wheat Triticum aestivum increases with crop density and spatial uniformity. *Journal of Applied Ecology*, *38*(4), 784–790. https://doi.org/10.1046/j.1365-2664.2001.00634.x

Wit, M. de, Kegge, W., Evers, J. B., Vergeer-Van Eijk, M. H., Gankema, P., Voesenek, L. A. C. J., & Pierik, R. (2012). Plant neighbor detection through touching leaf tips precedes phytochrome signals. *Proceedings of the National Academy of Sciences of the United States of America*, *109*(36), 14705–14710. https://doi.org/10.1073/pnas.1205437109

Xue, Y., Xing, J., Wan, Y., Lv, X., Fan, L., Zhang, Y., Song, K., Wang, L., Wang, X., Deng, X., Baluška, F., Christie, J. M., & Lin, J. (2018a). Arabidopsis Blue Light Receptor Phototropin 1 Undergoes Blue Light-Induced Activation in Membrane Microdomains. *Molecular Plant*, *11*(6), 846–859. https://doi.org/10.1016/j.molp.2018.04.003

Xue, Y., Xing, J., Wan, Y., Lv, X., Fan, L., Zhang, Y., Song, K., Wang, L., Wang, X., Deng, X., Baluška, F., Christie, J. M., & Lin, J. (2018b). Arabidopsis Blue Light Receptor Phototropin 1 Undergoes Blue Light-Induced Activation in Membrane Microdomains. *Molecular Plant*, *11*(6), 846–859. https://doi.org/10.1016/j.molp.2018.04.003

Yang, C., & Li, L. (2017). Hormonal regulation in shade avoidance. *Frontiers in Plant Science*, *8*(September), 1–8. https://doi.org/10.3389/fpls.2017.01527

Yang, X., Boateng, K. A., Strittmatter, L., Burgess, R., & Makaroff, C. A. (2009). Arabidopsis separase

functions beyond the removal of sister chromatid cohesion during meiosis. *Plant Physiology*, *151*(1), 323–333. https://doi.org/10.1104/pp.109.140699

Zhao, F., Du, F., Oliveri, H., Zhou, L., Ali, O., Chen, W., Feng, S., Wang, Q., Lü, S., Long, M., Schneider, R., Sampathkumar, A., Godin, C., Traas, J., & Jiao, Y. (2020). Microtubule-Mediated Wall Anisotropy Contributes to Leaf Blade Flattening. *Current Biology*, 3972–3985. https://doi.org/10.1016/j.cub.2020.07.076

6 Supplemental Figures

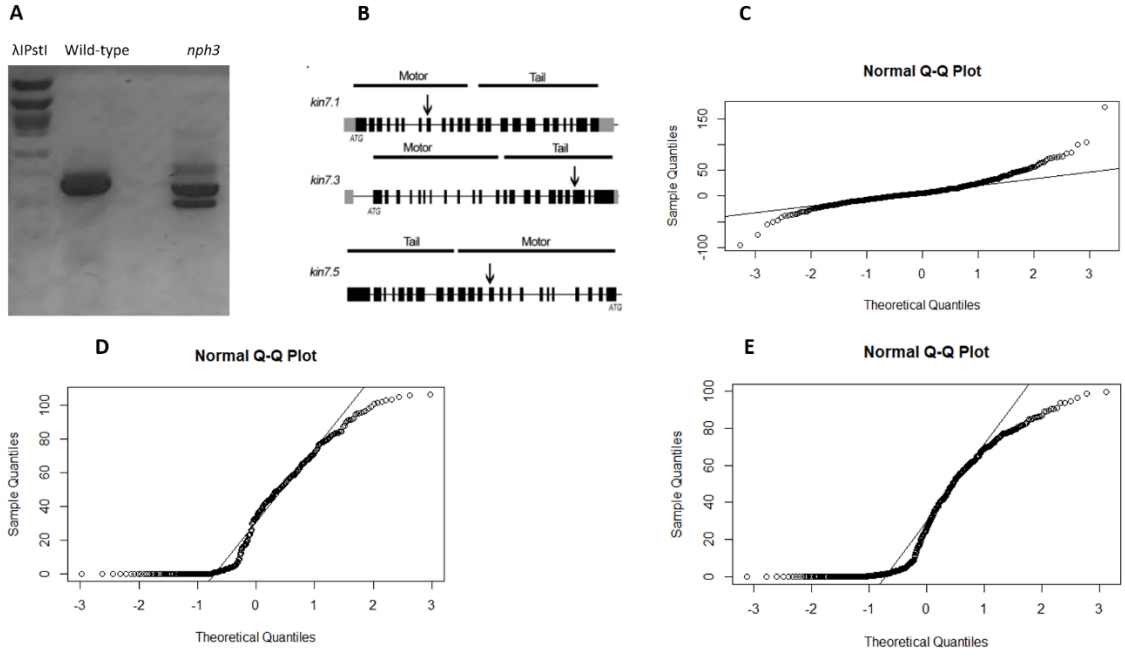

Figure S 1 Supplemental figures for physiological experiments. (A). *nph3* genotyping. PCR products resulted from multiplex PCR using genomic DNA extracted from Col-0 (wild-type) and *nph3* mutant line. Primers used: LBb1.3 (ATTTTGCCGATTTCGGAAC,), LP (TTTTTGCATTTGTTCCCAGAC), RP (TGAGTGTTTGCTGAATGATGC). Primers design: as described in http://signal.salk.edu/tdnaprimers.2.html. (B). Position of T-DNA insertion sites in *kin7.1*, *kin7.3*, *kin7.5* (Moschou et al., 2016). (C) Normal probability QQ-plot (quantile-quantile plot) for hypocotyl growth rates. The input consists of all the values (hypocotyl lengths) resulted from all replicates and genotypes. (D). QQ-plot for values used for the phototropism control assay (Figure 16A). (E). QQ-plot for values used for phototropism assay (Figure 16B).

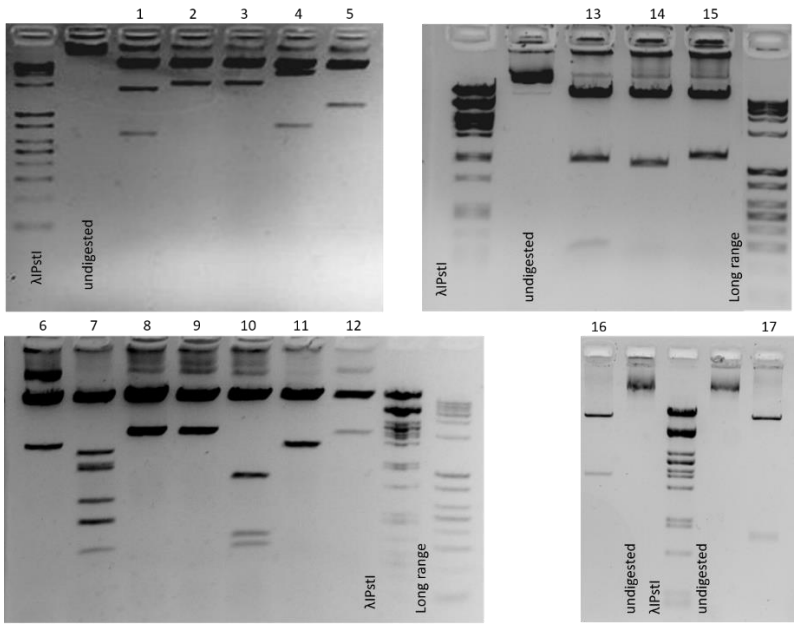

Figure S 2. Restriction-digestion validation in 1.2% agarose gel electrophoresis of the TAP-plasmids. 1. LRR (At1g49750.1), 2. LRR (At3g20820), 3: Calmodulin-binding protein (At4g33050.2), 4: FHY3 (At3g22170.1), 5: LSM8

(At1g65700), 6: SEC31B (At3g63460), 7: SRP72 (At1g67680), 8: CRCK2 (At4g00330.1), 9: UBA2C (At3g15010), 10: Alpha-L-Binding (At5g15750), 11: emp24 (At3g22845), 12: Calmodulin-binding protein (At4g33050.2), 13: CALM6 (At5g21274.1), 14: LSM5 (At5g48870), 15: LSM8 (At1g65700), 16: RGGB (At4g17520), 17: RGGA (At4g16830). All digestions were done using HindIII.

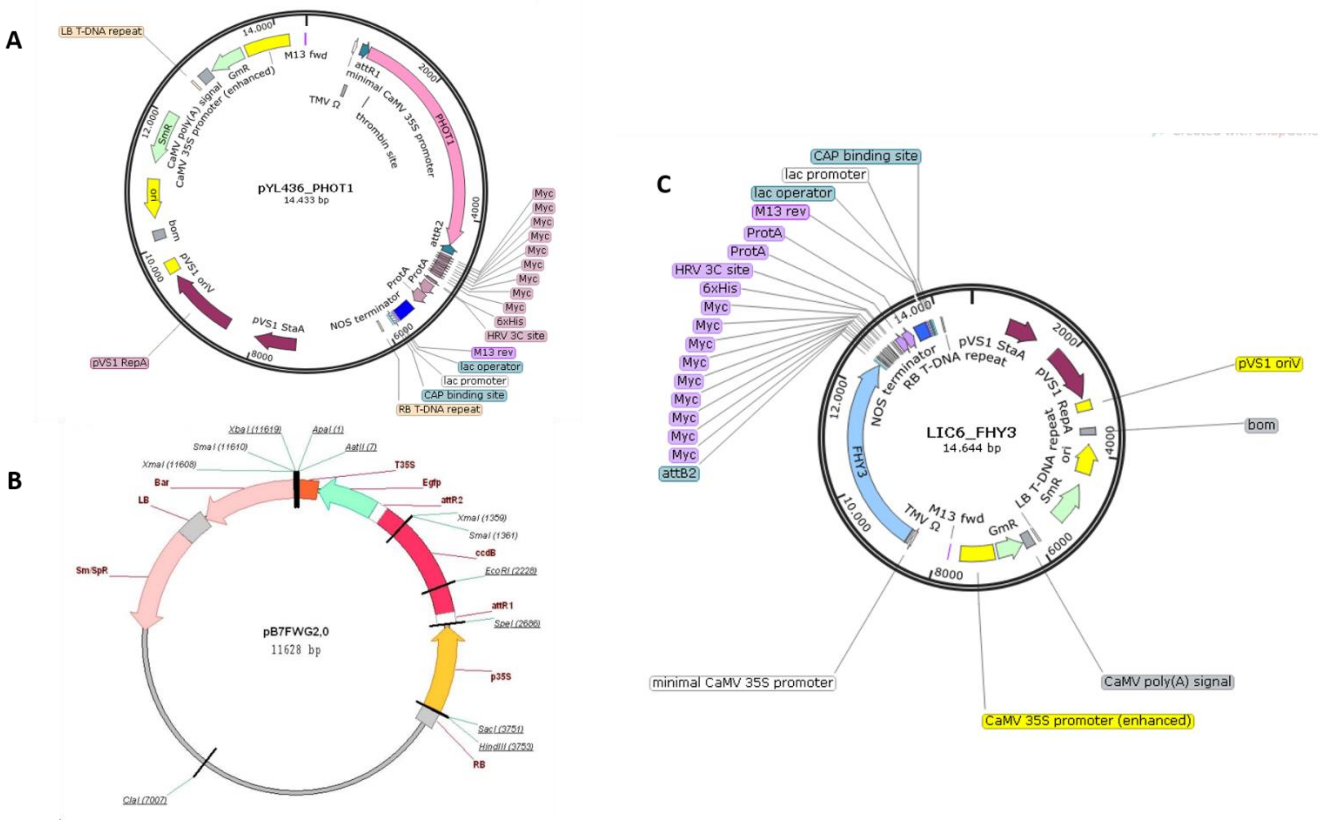

Figure S 3. Plasmid maps of constructs used to validate interactions between YFP-Kin7.3t and PHOT1 or FHY3. All vectors used to transform *Agrobacteria* (strain: Gv3101), which then used for transient expression of the protein in *N. benthamiana* leaves (agroinfiltration) (A): phot1 cDNA had been cloned into pYL436-TAP vector with Gateway technology (unknown entry Gateway vector). (B) pB7FWG2,0 carrying green fluorescent protein gene (Egfp), driven by 35S promoter (Karimi et al., 2002) (C): fhy3 genomic DNA had been cloned into LIC6-TAP vector with Gateway technology (unknown entry Gateway vector). Figures A and C made using SnapGene and they do not correspond to precise maps (unknown entry vector).

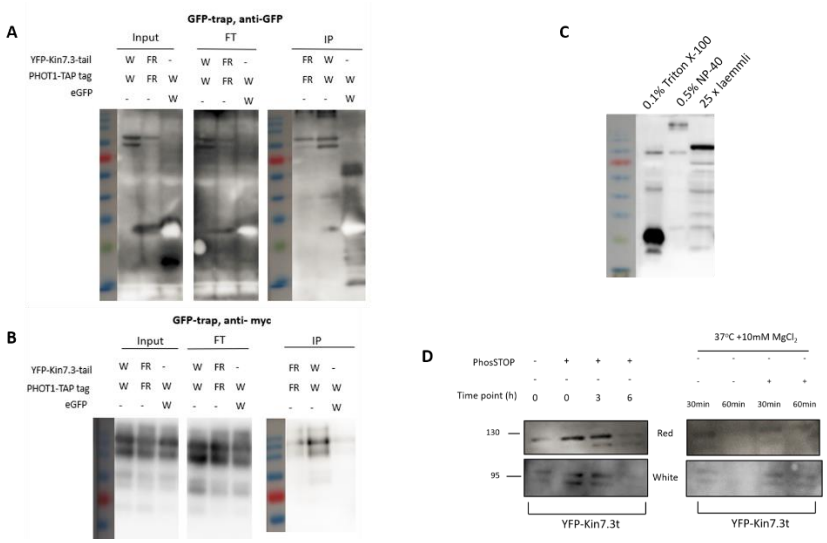

Figure S 4. (A, B, C): Row images after protein immunodetection on PVDF membranes. (A). Immunodetection of GFP and YFP-Kin7.3t proteins using anti-GFP antibody (B) Immunodetection of PHOT1-Tap-tagged protein using

anti-myc antibody. (C): Immunodetection of YFP-Kin7.3t using anti-GFP. Different lanes correspond to different detergents used in the extraction buffer. (D): Phosphorylation assay for YFP-Kin7.3t using phosphatase inhibitors (PhosSTOP) or Alkaline Phosphatase, Calf Intestinal (CIP). CIP is activated in 37°C, $MgCl_2$ was used to saturate EDTA (already added to the extraction buffer). Different time intervals used either for PhosSTOP or CIP assay in order to potentially observe different ratio between the two migrated proteins forms.